



Expertise
and insight
for the future

Seung-Goo Kim

Design of an Alarm System Using a Thermoelectric Generator

Metropolia University of Applied Sciences

Bachelor of Engineering

Electronics Degree Programme

Bachelor's Thesis

03 March 2019

| | |
|--|---|
| Author Title | Seung-Goo Kim Design of an Alarm System Using a Thermoelectric Generator |
| Number of Pages Date | 38 pages + 3 appendices 03 March 2019 |
| Degree | Bachelor of Engineering |
| Degree Programme | Electronics |
| Professional Major | |
| Instructors | Janne Mäntykoski, Senior Lecturer |
| <p>The goal of this project was to design a prototype that would operate by itself to detect wildfires in the deep forest. The device doesn't need a dependent power source or people to manage this device.</p> <p>The operation principle of this prototype would be to use some components such as a thermoelectric generator (TEG), an IR sensor, and a communication terminal. Put simply, even though there is no dependent power source (like a battery, electric wire) in the deep forest, it would be able to operate by itself using voltage from a TEG. The IR sensor would operate using voltage from the TEG, detect the temperature, and send an alarm message, if a wildfire were to break out in the forest.</p> <p>This prototype was developed using Arduino Uno with C code for microcontroller and the boost-converter evaluation module was used for amplifying the voltage to operate Arduino Uno.</p> <p>The main task to be solved by conducting this thesis work is to generate voltage using a TEG and transmitting the message. Therefore, the prototype was successful in relation to the first objective of the project.</p> <p>Finally, the overall objective of this paper is to contribute to the design of an alarm system that can be used to prevent big wildfires from developing.</p> | |
| Keywords | wildfire alarm prototype, thermoelectric generator, Seebeck Effect, IR sensor |

Contents

List of Abbreviations

| | | |
|-------|--|----|
| 1 | Introduction | 1 |
| 2 | Background of TEG | 2 |
| 2.1 | Basic Principle | 2 |
| 2.2 | Seebeck Effect | 3 |
| 2.2.1 | Basic Concept | 3 |
| 2.2.2 | Background of the Seebeck Effect | 4 |
| 2.2.3 | Emf and Ohm's Law | 5 |
| 2.2.4 | Relationship Between Ohm's Law, Current Density, and Emf | 7 |
| 2.2.5 | Thermoelectric Effect and Principle | 8 |
| 2.2.6 | Seebeck Coefficient | 9 |
| 2.3 | Calculating the Efficiency of ZT | 12 |
| 2.4 | Structure of a TEG | 13 |
| 3 | Background of IR Sensors | 15 |
| 3.1 | Basic Concept | 15 |
| 3.2 | Background of Infrared Radiation | 17 |
| 3.3 | Operation Principle of Infrared Thermometer Sensors Using a Thermopile | 19 |
| 3.4 | Structure and Operation of a Thermopile | 20 |
| 4 | Components of the Prototype | 21 |
| 4.1 | Thermoelectric Generator - TG12-6 | 21 |
| 4.1.1 | Connection Method | 23 |
| 4.2 | Infrared Sensor - MLX90614 | 24 |
| 4.3 | Telecommunication module - NRF24L01 | 25 |
| 5 | Design of the Prototype | 25 |
| 5.1 | Flow Diagram | 25 |
| 5.2 | 3D Structure | 27 |
| 5.3 | Arduino Wiring Diagram | 28 |
| 5.4 | Generated Voltage and Current | 29 |
| 5.5 | Circuit of the Prototype | 32 |

| | | |
|-----|--|----|
| 6 | Practical Point of View | 33 |
| 6.1 | Cost Analysis of the Prototype | 33 |
| 6.2 | Strengths and Weaknesses | 34 |
| 6.3 | Next Version | 36 |
| 7 | Conclusion | 38 |
| | References | 40 |
| | Appendices | |
| | Appendix 1. Transmitting Code | |
| | Appendix 2. Receiving Code | |
| | Appendix 3. Structure of the Prototype | |

List of Abbreviations

| | |
|-------|-------------------------------------|
| TEG | Thermoelectric Generator |
| emf | Electromotive Force |
| FSK | frequency-shift keying |
| IR | Infrared Sensor |
| FOV | Field of View |
| PWM | Pulse Width Modulation |
| SMBus | System Management Bus |
| ZT | Index of efficiency of TEG material |

1 Introduction

Almost every summer in the dry season, lots of wildfires have broken out along the border between Russia and Finland, particularly in Lapland [1]. Even though the range covered by the wildfire alarm system keeps expanding, there are still many places which can't be covered by an alarm system because there are no electrical lines. This means that cameras or sensors cannot be used due to the absence of an electrical source. All of the electric sensing systems, for example infrared (IR) cameras, sensors and so on, need an electrical source such as a battery. One of the reasons for the difficulty of suppressing wildfires at an early stage is late recognition caused by the lack of coverage due to the absence of an electrical source.

The goal of this study was to make a prototype for a wildfire alarm without an electrical source such as an electricity line, or a voltage source such as a battery. It would use a battery charging system using harvested energy.

The basic concept of this thesis is how to use harvested energy for the achievement of Early Suppression, Fast Response (ESFR). In recent years, growing investment in harvested energy experiments is resulting in more efficiency. Along with these experiments and the development of technology, the method or use or application of energy that is transformed from nature also keeps advancing. This would include, for example, photovoltaics, Moonie harvesters using piezoelectric materials, and battery chargers using integrated radio frequency technology [2]. Above all, converting from natural energy to electrical energy in order to supply power for consumer electronics is a popular topic.

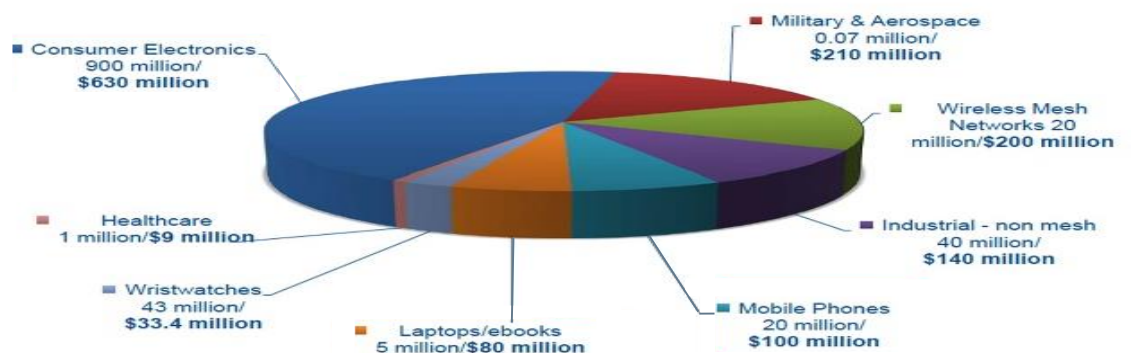


Figure 1. Energy harvesting market in 2017 [2]

As Figure 1 shows, in recent years, a lot of energy harvesting technology has been developed to convert from natural energy to electrical energy. Among these recent technologies, this thesis will focus on the “Thermoelectric Generator (TEG)” method for converting energy. This is also called a “Seebeck generator”, which is a solid-state device that converts heat flux (temperature differences) into electrical energy through a phenomenon called the “Seebeck effect”.

2 Background of TEG

2.1 Basic Principle

In 1821, Thomas Johan Seebeck recognized that a thermal gradient formed between two dissimilar conductors can produce electricity. The main basic principle of TEG is the fact that a temperature gradient in two semiconductors causes the diffusion of charge carriers. As shown in Figure 2, this will produce electricity in two sides where one side is the hot side and the other side is the cold side.

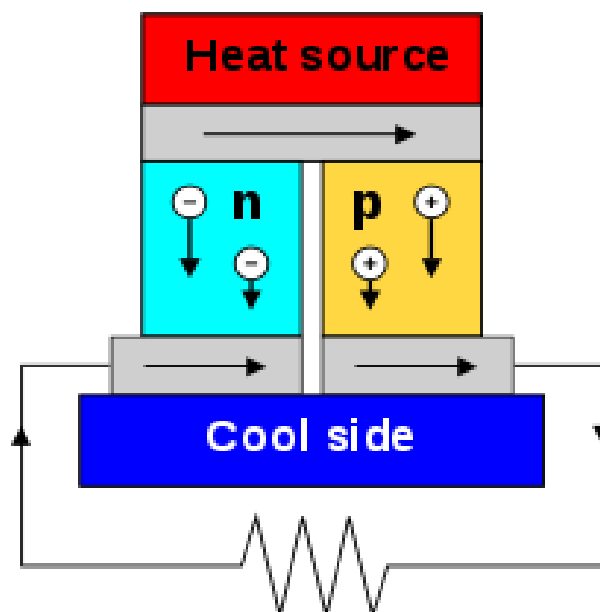


Figure 2. Circuit of TEG composed of n-dope and p-dope semiconductor [3]

This is called the “Seebeck effect”. The Seebeck effect is a phenomenon in which a temperature difference between two dissimilar electrical conductors or semiconductors

produces voltage. When heat is applied to one side of a semiconductor, heated electrons flow toward the cold side and then if the pair is connected through an electric circuit, direct current (DC) flows through the circuit.

2.2 Seebeck Effect

2.2.1 Basic Concept

To put it simply, the Seebeck effect is the effect that converts heat energy (natural energy) to electrical energy. The basic concept of the Seebeck effect starts from a thermocouple. A thermocouple is known for three effects: the Seebeck effect, the Peltier effect, and the Thomson effect, all named after the respective scientist who made their discoveries in the period 1822~1847. In the Seebeck effect, when two dissimilar wires of conductor or semiconductor are joined together and heat is applied to the two joints, the current flows in a closed loop. And if the closed loop is broken and if the voltage can be measured in the broken part, it is called "Seebeck Voltage". [4]

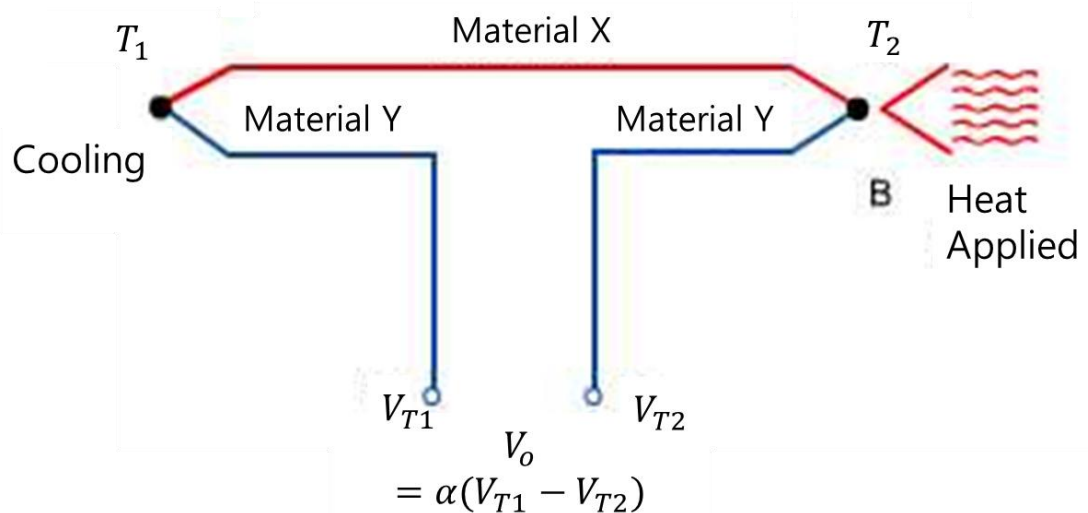


Figure 3. Simple Seebeck voltage [5]

As shown in Figure 3, Seebeck voltage is made by the difference in temperature (T_1 and T_2) at two joints. However, if the temperature of the two parts is the same, V_{T1} and V_{T2} , it means that V_o equals zero. The interaction between thermal energy and electrical energy is based on temperature difference.

2.2.2 Background of the Seebeck Effect

When the end of a thermocouple is heated up, electrons in the warmer side diffuse toward the colder side. Consequently, the electromotive force (emf) is generated as well as current. The diffusion of electrons in metal is made by free charge carriers such as free electrons and free holes. To understand the Seebeck effect, let us first see how electrons operate depending on temperature in a chemical equation. The principle of the Seebeck effect derived from classical theory, i.e., 'Electron Gas' by Drude in 1900. The theory was later expanded by Lorentz who published 'Kinetic Theory of Gases to the Free Electron Gas in a Metal'. It resulted in the 'Maxwell-Boltzmann Distribution' curve which showed that electrons would possess a range of speeds distributed about the mean velocity \bar{v} along with the temperature of the molecule.[7]

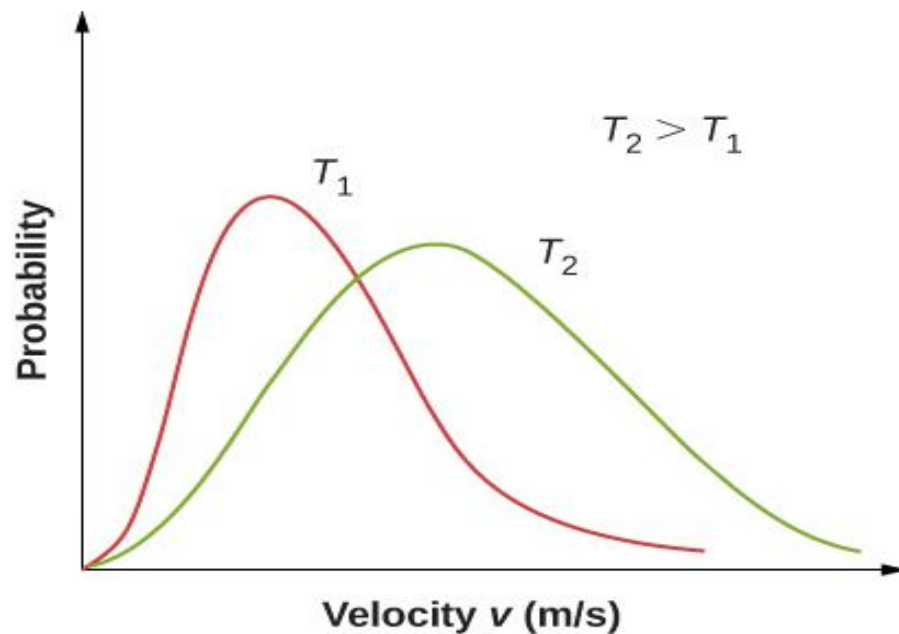


Figure 4. Maxwell-Boltzmann distribution [6]

As Figure 4 shows, electrons at a higher temperature have a higher probability of having a higher velocity than at a lower temperature. The equation of the number of moving molecules for which velocity is from v to $v + dv$ is expressed as:

$$n(v) = Av^2 T^{-3/2} e^{\left(\frac{-Bv^2}{T}\right)} dv \quad (1)$$

where A and B are constant, v is mean velocity, and T is the temperature of the molecule. If temperature is increased, the maximum and mean velocities shift to higher values and

the Maxwell-Boltzmann curve flattens out. This means that the probability of the molecule having a high velocity increases. If the temperature is reduced to zero, the mean velocity would be zero.

Since the Seebeck effect is the most important part of this project, this section will explain the Seebeck effect in detail, elaborating some concepts from Ohm's law and emf as thoroughly as possible.

2.2.3 Emf and Ohm's Law

Electromotive force (abbreviated 'emf') is the energy per unit charge. Simply put, it means that a unit charge moves from low potential to high potential by emf. The SI unit of emf is joules/coulomb (J/C) and it is the same as volt (V).

Before trying to understand emf in electrical components, let's look at it first with a voltaic cell. In a voltaic cell, current producing chemical reactions drive electrical charges across the electrolyte, connecting two wires to Zn, Cu and a voltage meter as shown in Figure 5. One electrode is put in a bottle which has an excess of charge and the other in a bottle with a deficit of charge. It shows that electrodes tend to oppose the current flow by moving electrons. At the electrode, the electrode-electrolyte interface serves as a 'pump' for moving electrons with pumping power. This corresponds to what happens with emf in contact electricity when there are chemical reactions at the electrode-electrolyte interfaces that provide the source of emf.

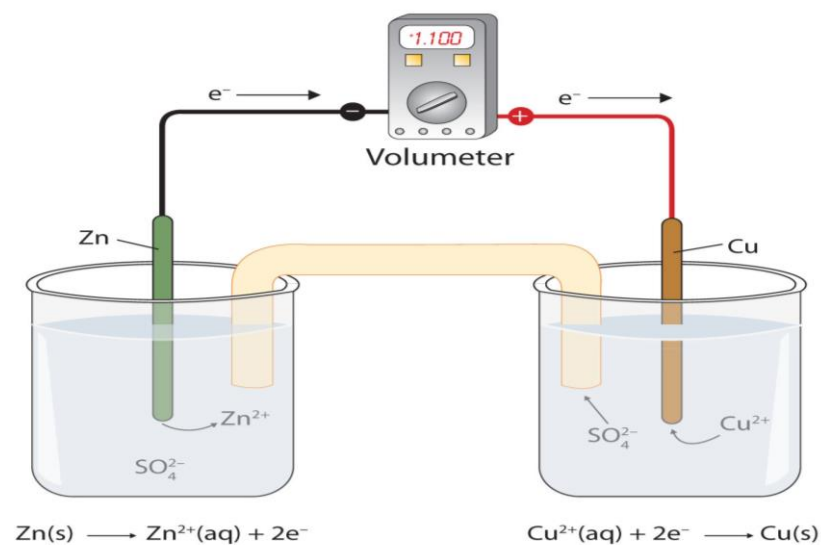


Figure 5. Redox reaction in a voltaic cell [7]

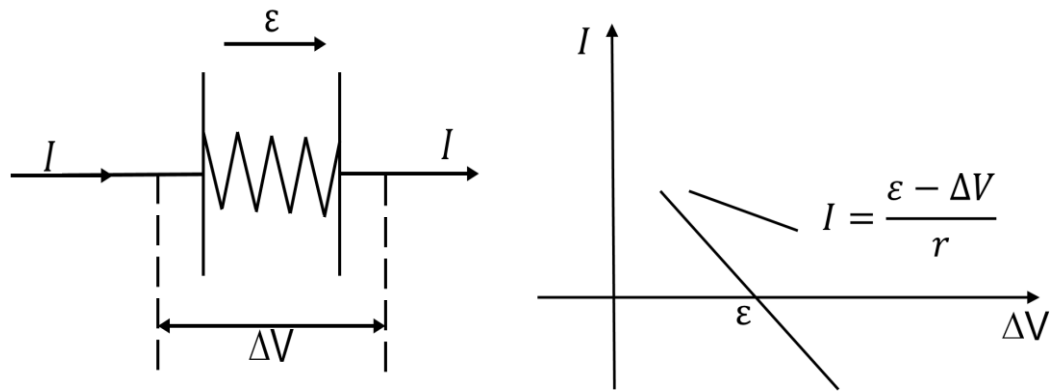


Figure 6. (a) Structure of internal resistance between two electrodes; (b) Current versus voltage differences for a source of emf [8]

As shown in Figure 6, if we see a small deviation of ΔV from (ϵ) , charge $dQ = Idt$ enters the source of emf at the left edge of the resistor and an equal charge come out the right. This means that internal resistance(r) has the same role as the electrolyte of a voltaic cell. Emf operates to raise the voltage across the cell by " ΔV " because of internal resistance so that the potential electrical energy of the charge dQ increases by ΔVdQ .

Along with raising the voltage, emf also provides Joule heating energy $I^2r dt = IrdQ$. So, in total, emf provides potential energy of both charge and heat energy.

Hence,

$$dQ = Idt, \text{ so } rdQ = I \times rdt$$

$$rdQ = Vdt = \Delta V$$

$$DdQ = \Delta VdQ + IrdQ$$

$$\mathbf{D = \Delta V + Ir} \quad (2)$$

On an open circuit, $I = 0$ is defined as the emf(ϵ) of the cell. When $\epsilon = \Delta V$, the current $I = 0$. However, when $\Delta V \neq \epsilon$, a cell can drive an electrical current.

Since the strength of emf D must be consistent with $\Delta V = \epsilon$ for $I \rightarrow 0$, it can be deduced that $D = \epsilon$. So, eq. (2), can be expressed as given by:

$$\mathbf{\epsilon = \Delta V + Ir} \quad (3)$$

From the above equation, current I can be obtained as

$$I = \frac{\varepsilon - \Delta V}{r} \quad (4)$$

In eq. (4), component r , ΔV and I can all be varied in a complex source of emf. This equation is used to define the basic concept of thermoelectric devices.[9]

2.2.4 Relationship Between Ohm's Law, Current Density, and Emf

If a wire does not have uniform temperature, it has a temperature gradient, so the wire has a tendency for the electrons to drift to the higher temperature. Thus, it becomes partly electrical $\sigma(\vec{E})$ and partly nonelectrical $\sigma(\vec{E}')$. So, Ohm's law local form $\vec{J} = \sigma\vec{E}$ can be generalized as given in the following equation:

$$\vec{J} = \sigma(\vec{E} + \vec{E}') \quad (5)$$

Eq. (6) corresponds to the local current density with emf which comes out when a TEG operates.

$$\vec{J} = \sigma(-\Delta V + E_{emf}) \quad (6)$$

where V is local voltage and σ is local conductivity. And E_{emf} is described generally as $E_{emf} = -S\Delta T$ (as part of the Seebeck effect), where S is the Seebeck coefficient and ΔT is the temperature difference.

2.2.5 Thermoelectric Effect and Principle

As shown in Figure 7, where there is a non-uniform temperature across the material of a device (or if the device is composed of two different materials), it produces a voltage difference between its ends which are split into two pieces, even though there is no current flow. This effect is called the Thermoelectric Effect. The phenomenon is caused by the different diffusion speeds of electrons in the two materials

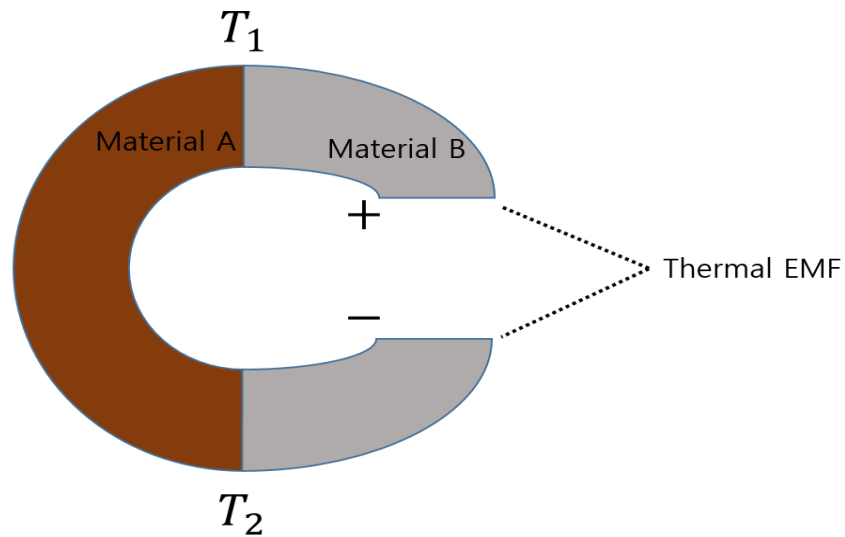


Figure 7. Thermal emf made by temperature gradients in different materials

. So, it creates a potential difference which is referred to as emf between the two junctions.

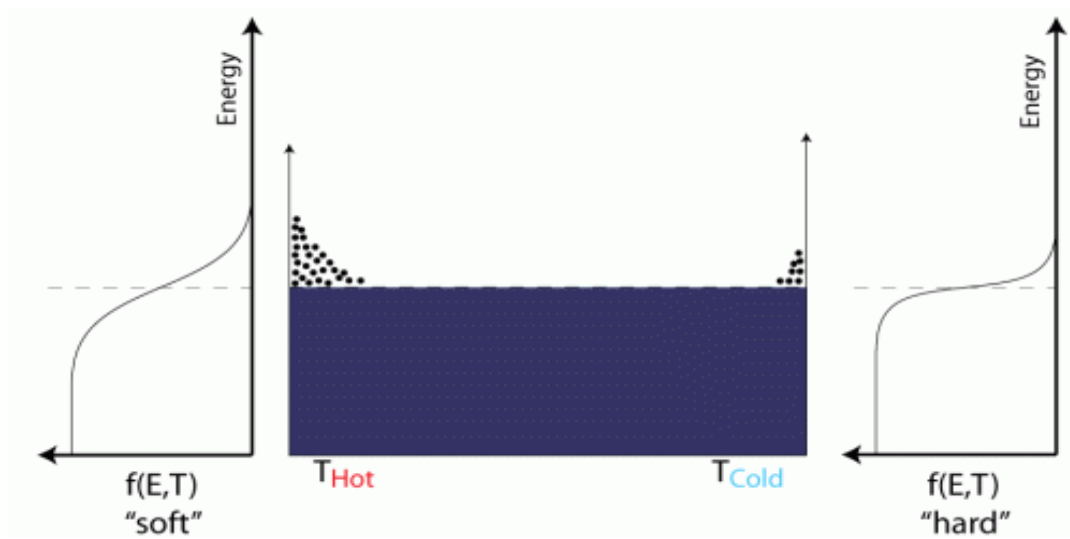


Figure 8. Energy diagram of a metal [10]

As shown in Figure 8, the hot side of a metal has a higher concentration of electrons than the cold side because the molecule which has a higher temperature has a higher probability of high velocity of molecule by eq. (1).

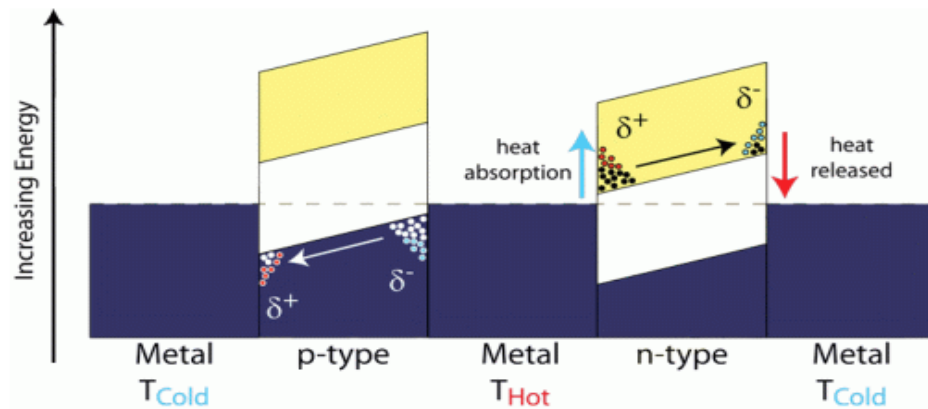


Figure 9. Electrons moving according to different temperatures [10]

As shown in Figure 9, non-equilibrium is always trying to establish an equilibrium situation, so the electron which has a higher temperature moves to the low temperature side by diffusion. As a result, voltage is generated.

2.2.6 Seebeck Coefficient

The Seebeck effect is affected by many factors, among them: voltage, temperature, and the material of the TEG.

The Seebeck coefficient is also known as thermopower, thermoelectric power, and thermoelectric sensitivity. The Seebeck coefficient of a particular material is a measure of the magnitude of an induced thermoelectric voltage in response to temperature difference across the material, as induced by the Seebeck effect. The SI unit of the Seebeck coefficient is volt per kelvin (V/K).[11] Namely, the ratio between the voltage difference induced and the temperature difference is called the Seebeck coefficient.

$$\alpha = -\frac{\Delta V}{\Delta T} = -\frac{V_{hot} - V_{cold}}{T_{hot} - T_{cold}} \quad (7)$$

If we make a component using only one material, there is no different potential and as a result there is no voltage. Therefore, the Seebeck coefficient cannot be measured directly. This is because the number of the coefficient is a relative number between the two materials which make up the component. In Table 1, the relative Seebeck coefficient was measured depending on different material combinations.

Table 1. Relative Seebeck coefficients for some material combinations [12]

| Materials | Relative Seebeck coefficient at 25°C [$\mu\text{V}/^\circ\text{C}$] | Relative Seebeck coefficient at 0°C [$\mu\text{V}/^\circ\text{C}$] |
|---------------------------------|---|--|
| Copper/constantan | 40.9 | 38.7 |
| Iron/constantan | 51.7 | 50.4 |
| Chromel/alumel | 40.6 | 39.4 |
| Chromel/constantan | 60.9 | 58.7 |
| Platinum (10%)/rhodium-platinum | 6.0 | 7.3 |
| Platinum (13%)/rhodium-platinum | 6.0 | 5.3 |
| Silver/palladium | 10 | |
| Constantan/tungsten | 42.1 | |
| Silicon/aluminum | 446 | |
| Carbon/silicon carbide | 170 | |

The Seebeck effect results from the temperature dependence of the 'Fermi energy' E_f , and the total Seebeck coefficient for nondegenerate n-type silicon is given by:

$$\alpha_s = -\frac{k}{q} \left[\ln\left(\frac{N_c}{n}\right) + 2.5 + s_n + \varphi_n \right] \quad (8)$$

where N_c is conduction band density, n is electron density (determined by doping concentration), k is the Boltzmann constant, and s_n is the exponent describing the relation between the relaxation time and the charge-carrier time. Relaxation time indicates the time between mean free time and collisions. The factor φ_n denotes the phonon drag effect (phonons dragging charge carriers towards the cold part of the crystal). This expression also can apply to p-type silicon except that the sign is positive instead of negative.

[13]

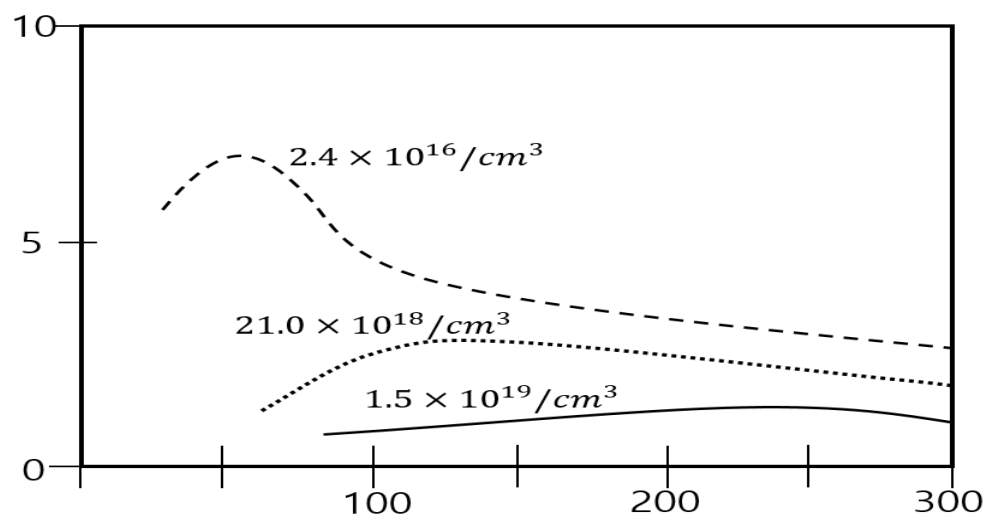


Figure 10. Seebeck coefficient of p-type silicon for three different doping concentrations [13]

As shown in Figure 10, we can also calculate via the other way using the Fermi level difference and the state of the mobile charge carriers. This expression is given by:

$$S = \frac{\int (E - E_F) \sigma(E) dE}{eT \int \sigma(E) dE} \quad (9)$$

which means that the energy of a state by heat $E - E_F$ is weighted by its contribution to conductivity and divided by unit charge and temperature.

In eq. (9),

$$\sigma(E) = e \times n(E) \times \mu(E) \quad (10)$$

where e is unit charge, $n(E)$ is total density of the carrier derived by summing the number of doping carriers and the number of material carriers, and $\mu(E)$ is the mobility of the carriers.[14]

2.3 Calculating the Efficiency of ZT

If we connect two components which are p-type and n-type semiconductors and heat up the warmer side of each device such that $\Delta T = T_h - T_c$, then the electrons in the n-type and the holes in the p-type will be heated up so total energy will go up. In the n-type component, electrons move to the low temperature part. On the other hand, in the p-type component, holes move to the low temperature part. As a result, in the n-type semiconductor, the low temperature part will be charged minus and the high temperature part will be charged plus. On the other hand, in the p-type semiconductor, it will work in reverse. This is how to operate the Seebeck effect in a TEG and we can calculate the efficiency of the thermoelectric material. This equation is given by:

$$Z = \frac{\alpha^2}{k \times \rho} \quad (11)$$

where Z is the thermoelectric material's figure of merit, α is the Seebeck coefficient, ρ is electrical resistivity and k is total thermal conductivity. If we multiply this eq. (11) by temperature T , the expression of a p/n type semiconductor is given by:

$$ZT = \frac{\alpha^2 T}{k \times \rho} = \frac{(S_p - S_n)^2 T}{\left[\rho_n k_n^{\frac{1}{2}} + \rho_p k_p^{\frac{1}{2}} \right]^2} \quad (12)$$

$$T = \frac{T_h + T_c}{2}$$

Currently, a thermoelectric material with $ZT=1$ is considered good, and a material with $ZT=3-4$ is an essential element of a TEG device.[15]

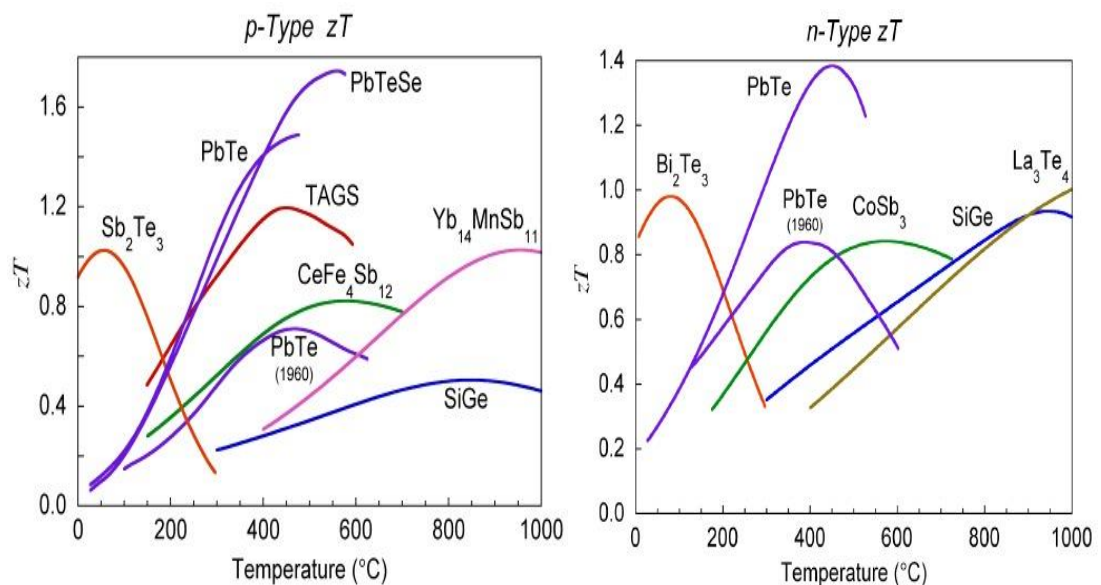


Figure 11. Comparison of ZT of p-type and n-type for various materials [16]

As shown in Figure 11, all materials have a different ZT value depending on temperature and how the material is doped as p-type and n-type. Also, there is an upper limitation of ZT because of the temperature limitation of the materials. Thus, there is the fact that any single material can be identified as the best for a particular operation range. Therefore, specific materials should be selected for different applications in order to operate in an appropriate range based on the situation.

2.4 Structure of a TEG

A TEG is a solid-state device that converts temperature differences directly into electrical energy.

Basically, as shown in Figure 12, a TEG uses doped semiconductors which are n-type and p-type. If we connect an n-type and a p-type semiconductor to each other and then apply temperature difference between the two sides, as mentioned in the previous section, the n-type part is charged minus by electrons and the p-type part is charged plus by holes as a result of the Seebeck effect. So, in the n-type part, current will flow to the upper part; however, in the p-type part, current will flow to the lower part. If we connect the load, the current will flow inside of the circuit so power will be generated.

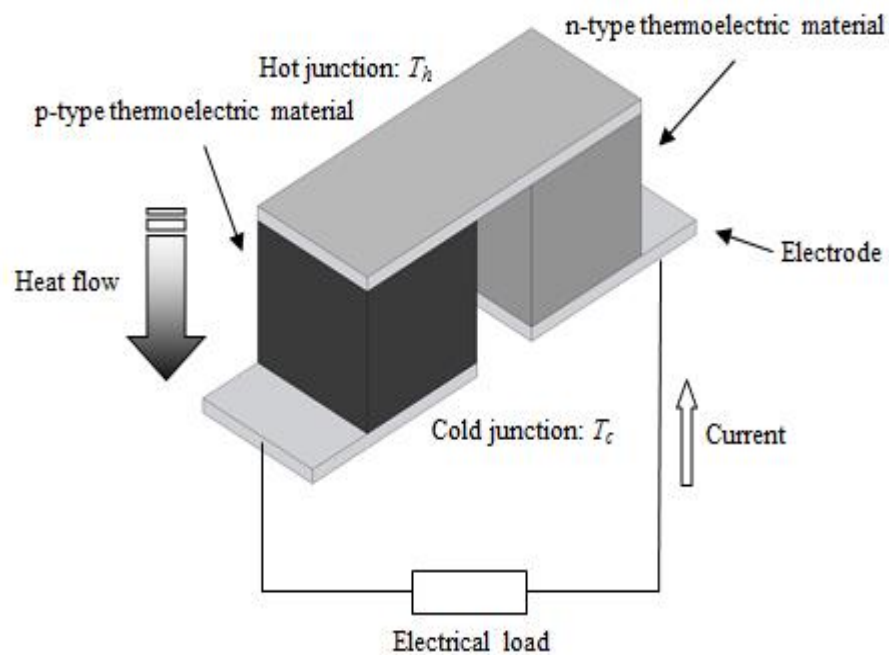


Figure 12. Basic structure of a practical TEG [17]

In practice, a TEG is made with multiple pellets of doped semiconductors which consist of n-type and p-type, in order to get more current flow and voltage. This is shown below in Figure 13.

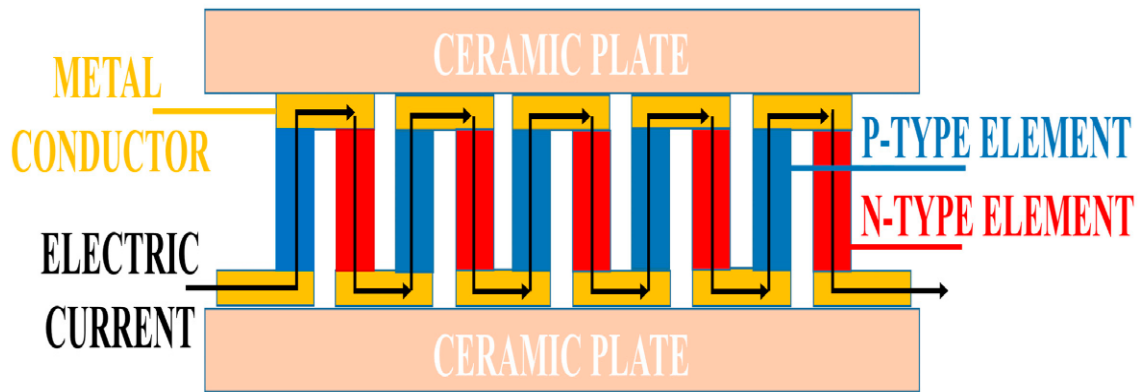


Figure 13. Multiple pellets of a doped semiconductor [18]

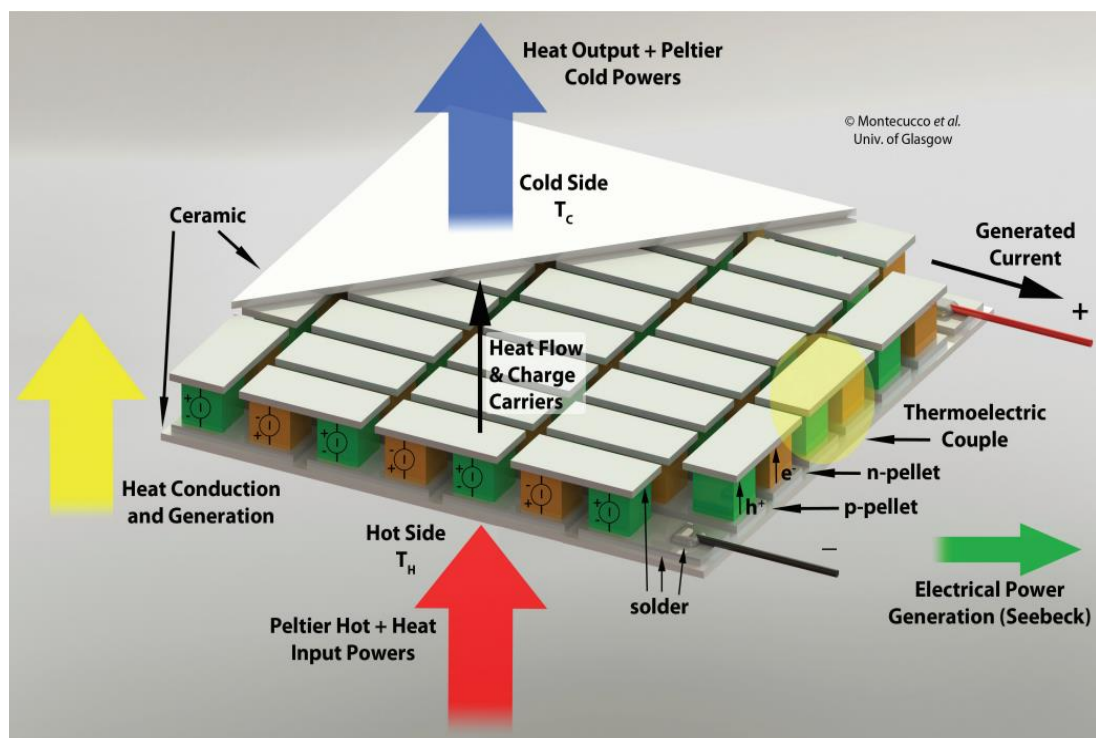


Figure 14. 3-D model of a TEG showing the main physical effects [19]

Figure 14 shows a 3D cut-away isometric drawing of a TEG module in which thermal energy is applied on the bottom surface. Externally applied thermal energy (which is usually heat from a heat source such as a wildfire in this thesis) is conducted through the module while additional heat is generated (Joule heating) inside the module and pumped (Peltier effect) through the hot and cold sides as indicated by the coloured arrows. [19] Multiple pellets of p-type and n-type semiconductors are connected electrically in a series. The voltage from each pellet is added such that the generated voltage is higher.

3 Background of IR sensors

3.1 Basic Concept

Recently, there has been a lot of research and development of thermal detectors. As a result, not only is the size of the chip and the sensor getting smaller, but the price is getting cheaper as well. Many applications have been developed using sensors such as cameras for detecting burglary, fire alarm systems, and even military equipment. In Korea, almost all cars have a 'Black Box' installed for recording evidence when accidents happen. This 'Black Box' has a thermal detector for use at night. So, the number of applications for thermal detectors is countless and more are still being developed.

The basic principle of the thermal detector is the absorption of thermal radiation. Thermal radiation is one of the mechanisms which transfer heat. All material emits electromagnetic radiation generated by the thermal motion of charged particles if the material temperature is greater than absolute zero. The thermal object emits infrared electromagnetic radiation which is converted into thermal energy and the thermal detector detects the electromagnetic radiation.

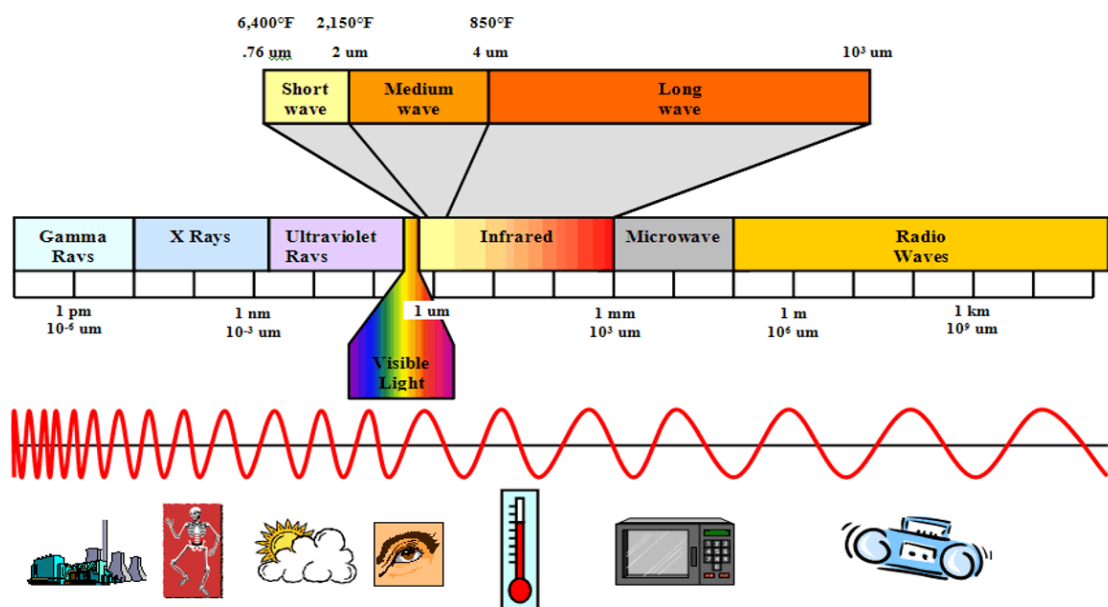


Figure 15. Infrared spectrum and wavelength [20]

As shown in Figure 15, a human being can only detect a narrow range of wavelength, called visible light, which is from 400 nm to 700 nm. On the other hand, the range which is detected by a thermal detector, called infrared, is part of the invisible spectrum that has a longer wavelength of more than 800 nm. The range of the infrared spectrum is normally from 800 nm to 1 mm. It is the direct transfer of heat from a source of heat (such as a stove, a wood fire, or even the sun), without any mediator material. Likewise, most of the thermal radiation emitted by objects near normal environmental temperature (such as room temperature) is infrared.

3.2 Background of Infrared Radiation

Energy made by thermal radiation has different energy levels depending on the infrared wavelength. This means that each infrared wavelength has different energy and vice versa. The energy which is emitted is called radiant energy. The basic principle of radiant energy is the conversion of energy from thermal energy into electromagnetic energy. As mentioned in the introduction, all material which has a temperature greater than absolute zero emits infrared energy. Infrared is propagated by photons and if the temperature of the source goes up, the number of emitted photons will also increase. The characteristic of thermal radiation depends on the material of the surface because absorptivity, reflectivity, and emissivity are different.

A photon is propagated following Planck's law. Planck's law describes the spectral density of radiation emitted by a black body (perfect absorption and perfect radiation material) at a given temperature T . Planck's law shows that the quantity $B_\nu(\nu, T)$ is spectral radiance as a function of temperature and frequency.[21]

$$B_\nu(\nu, T) = \frac{2h\nu^3}{c^2} \frac{1}{e^{\frac{h\nu}{k_B T}} - 1} \quad (13)$$

where h is the Planck constant around $6.626 \times 10^{-34} \text{ J} \cdot \text{s/rad}$, ν is frequency at absolute temperature T , c is the speed of light (approximately 3.0×10^8), and k_B is the Boltzmann constant (approximately $1.38 \times 10^{-23} \text{ J} \cdot \text{K}^{-1}$). This expression shows that the amount of energy radiated per unit area depends on frequency. It can also be described in terms of wavelength or energy density in volume of radiation.

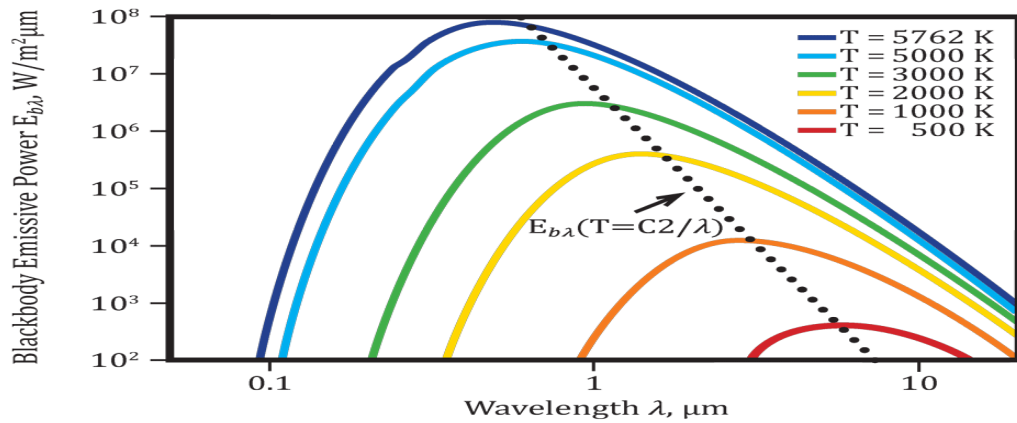


Figure 16. Blackbody emissive power spectrum [22]

Figure 16 is a graph which explains Wein's displacement law and presents the black body radiation spectrum based on eq. (14) for various temperatures. It shows the following two facts: first, the power of emission increases with temperature, and second, shorter wavelengths have more radiant energy. Plank's law also can be used to describe how temperature effects wavelength numerically in the expression. Start with eq. (14) which changes from frequency to wavelength λ as shown in eq. (15):

$$B_{\nu}(\nu, T) = \frac{2h\nu^3}{c^2} \frac{1}{e^{\frac{h\nu}{k_B T}} - 1} \quad (14)$$

$$B_{\lambda}(\lambda, T) = \frac{2hc^2}{\lambda^5} \frac{1}{e^{\frac{hc}{\lambda k_B T}} - 1} \quad (15)$$

Differentiating the equation with respect to wavelength λ and setting it equal to zero we get:

$$\frac{\partial B}{\partial \lambda} = 2hc^2 \left(\frac{hc}{kT\lambda^7} \frac{e^{\frac{hc}{\lambda kT}}}{\left(e^{\frac{hc}{\lambda kT}} - 1\right)^2} - \frac{1}{\lambda^6} \frac{5}{e^{\frac{hc}{\lambda kT}} - 1} \right) = 0 \quad (16)$$

$$\frac{hc}{kT\lambda} \frac{e^{\frac{hc}{\lambda kT}}}{e^{\frac{hc}{\lambda kT}} - 1} - 5 = 0 \quad (17)$$

By defining $x = \frac{hc}{\lambda kT}$,

$$\begin{aligned} \frac{x e^x}{e^x - 1} - 5 &= 0 \\ (x - 5)e^x + 5 &= 0 \\ \therefore x &= 4.965114 \text{ by Newton's method} \\ \lambda_{max} &= \frac{hc}{xkT} = \frac{2.897729 \times 10^6 \text{ mm} \cdot \text{K}}{T} \end{aligned} \quad (18)$$

Using eq. (18), it is proved that there is a relation between wavelength and temperature.

3.3 Operation Principle of Infrared Thermometer Sensors Using a Thermopile

The basic principle of a non-contact infrared thermometer is to measure emissions and calculate temperature using Plank's law. Emissivity is only affected by the temperature of the material surface, so an infrared thermometer measures the temperature of the surface only. Currently, thermal detectors are usually divided into four types: 'Bolometer', 'Pyroelectric', 'Pneumatic', and 'Thermopile'. Among these types, the MLX90614 is classified as a 'Thermopile' which has a heat sensing method using the Seebeck effect. As mentioned in the previous section, the output of the Seebeck effect is voltage created by an electric magnetic force made by temperature gradient.

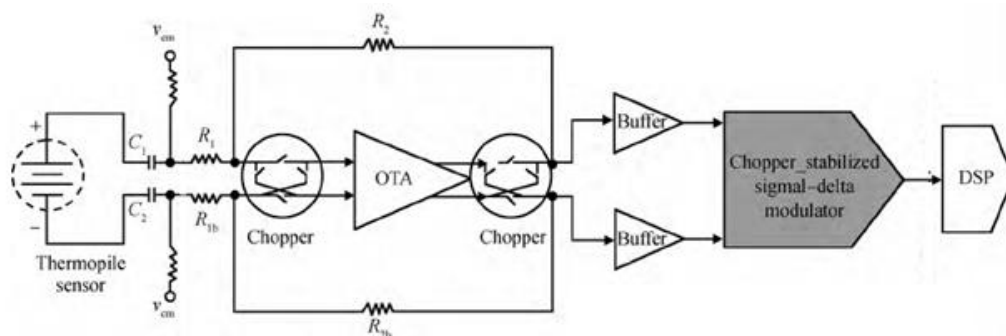


Figure 17. Structure of an infrared thermometer sensor [23]

An infrared thermometer consists of various components for converting from a radiant to an electrical signal. Among the various components, a thermopile sensor has the main role in a thermopile thermometer. As shown in Figure 17, the operation principle follows this given procedure. First, a thermopile sensor generates voltage. Second, a capacitor and a resistor operate as a filter to eliminate noise. Third, a chopper is used to supply stabilized current and eliminate low frequency error at OPamp. Fourth, an amplifier operates to amplify the voltage. And fifth, a final chopper, a final buffer, and a modulator are used to stabilize the output.

3.4 Structure and Operation of a Thermopile

In order to get high voltage output, a thermopile sensor must have many thermocouples that are connected serially on a substrate to magnify the temperature difference between the hot junction area and the cold junction area for the Seebeck effect.

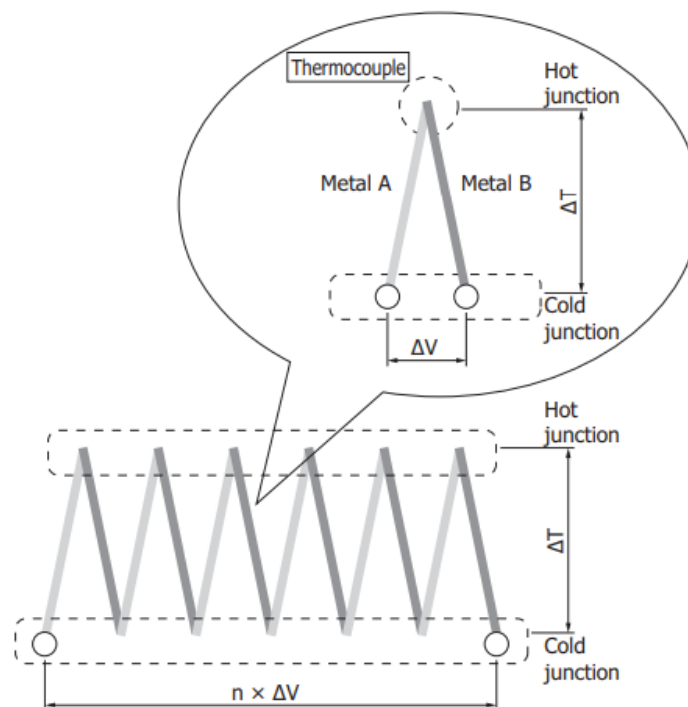


Figure 18. Principle of a thermal detector [24]

As shown in Figure 18, many thermocouples are connected serially and the number of connected thermocouples influences the characteristic of sensitivity and how much infrared emission can be converted into voltage. As shown in Figure 19, the thermopile

sensing part consists of two major areas. One is the thermocouple, and the other is the infrared absorption film.

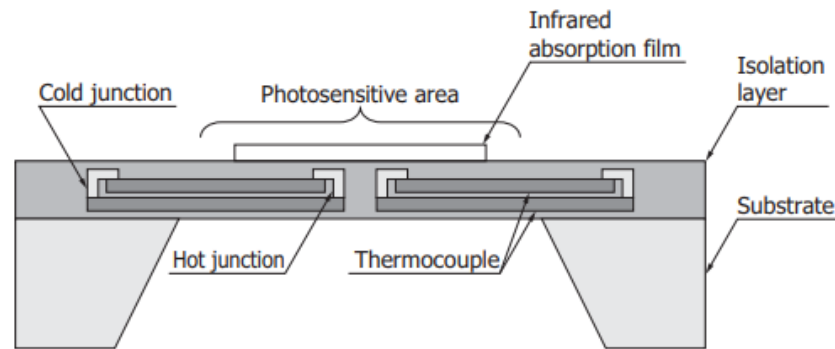


Figure 19. Structure of a thermal detector [24]

In Figure 19, if the infrared absorption film absorbs the infrared, temperature increases only at the hot junction of the thermocouple; this would then generate a temperature difference, and so finally, voltage would be generated by the electromagnetic force called the Seebeck effect.

Eq. (19) shows the sensitivity of a thermopile that is determined by the number of thermocouples.

$$R_v = \frac{\eta n \alpha}{G \sqrt{1 + \omega^2 \tau^2}} \quad (19)$$

where R_v is thermopile sensitivity, η is emissivity, n is the number of thermocouples, α is the Seebeck coefficient, G is the thermal conductivity of the conductor material which exists on the membrane, and ω, τ is the relation with emission of radiation.

4 Components of the Prototype

4.1 Thermoelectric Generator -TG12-6

Figure 20 shows the TEG produced by Marlow Industries. This is a single-stage thermoelectric generator, which means that a p-doped and an n-doped semiconductor are arranged in one stage.

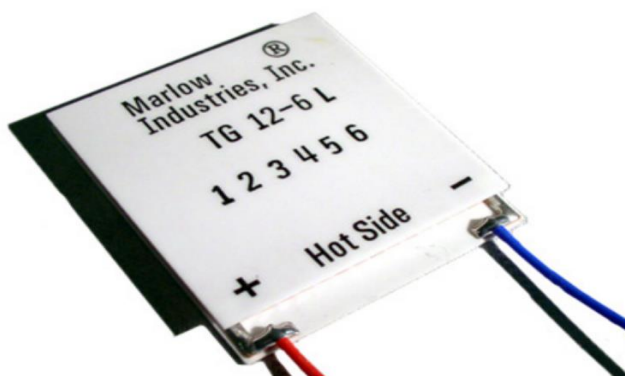


Figure 20. TG12-6 module [25]

For getting maximum reliability, continuous operation below 200°C is recommended. In addition, the upper limit at the hot side is 230°C and nominal ZT should be 0.73.

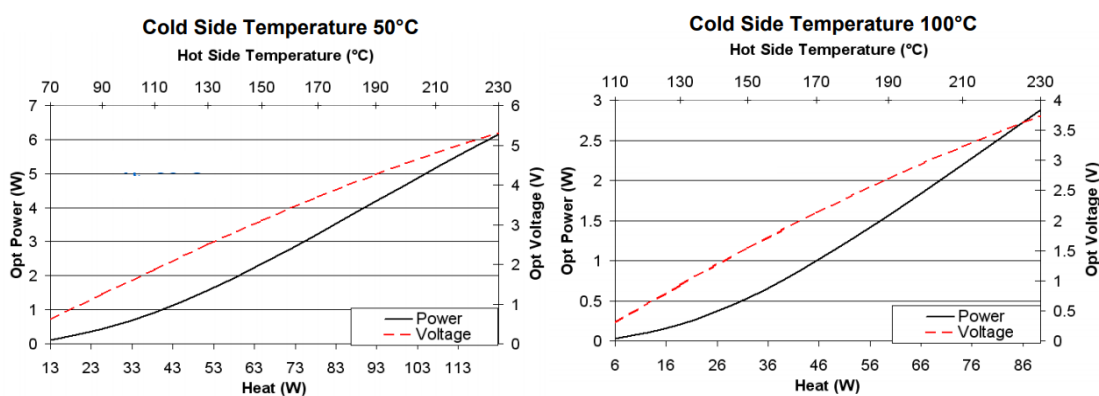


Figure 21. Output power and voltage comparison depends on cold side temperature [26]

As Figure 21 shows, output power and output voltage are generated differently depending on the cold side temperature. When the hot side temperature is 230°C and the cold side temperature is 50°C, the output voltage is above 5V. On the other hand, when the cold side temperature is 100°C, the output voltage is lower than 4V. This is due to the coefficient of the Seebeck effect. In order to get high output voltage, we have to determine how to make the temperature difference as great as possible. For getting more temperature difference between the hot side and the cold side, a heat sink is an appropriate tool for reducing the temperature at the cold side.



Figure 22. Heat sink [27]

Generally, as shown in Figure 22, heat sinks are made of aluminium because thermal conductivity is higher than other materials when comparison is based on price. High thermal conductivity means that it has high heat transferring capacity.

4.1.1 Connection Method

The recommended Arduino input voltage is about 7(V) to 12(V) and general input current is 1A. However, generally, the ZT of a commercial TEG is not enough to operate an Arduino. Furthermore, using only one TG12-6 is not enough to operate perfectly. Therefore, in this study, in order to get the required voltage, two TEGs are used for generating the voltage.

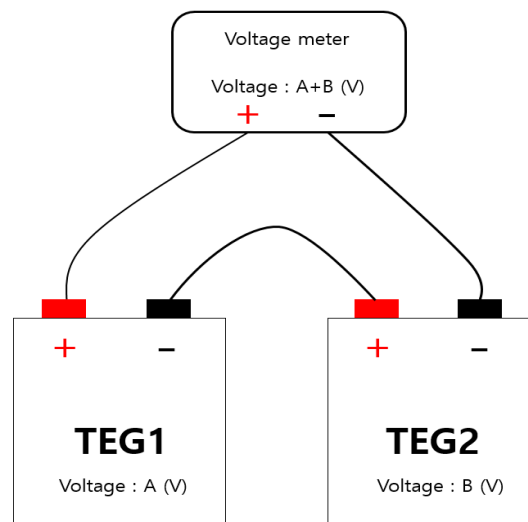


Figure 23. TEGs series connection

From a voltage point of view, as shown in Figure 23, a series connection is the same as summing the batteries in a series connection. If TEG1 generates voltage A, and TEG2

generates voltage B, the total voltage of the TEGs is A+B voltage. As a result, it can be used to operate the Arduino properly. However, from a current point of view, this connection method is not suitable. Since a boost-converter is only used for amplifying the voltage, the current problem becomes the main problem if the prototype components need a high current amount. At that time, the TEG would have to generate as much current as possible. Generally, the amount of current generated by a TEG is under 1[A]. So, the two TEGs have to be connected as shown in Figure 24.

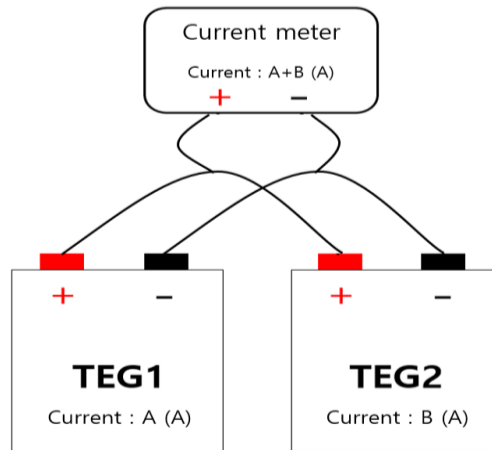


Figure 24. TEGs parallel connection

In parallel connection, if TEG1 generates current A, and TEG2 generates current B, the total current of the TEGs is A+B ampere.

4.2 Infrared Sensor- MLX90614

The MLX90614 is an infrared thermometer for a non-contact temperature sensor which is produced by the Belgian company Melexis. It has a high accuracy of 0.5°C and a wide detecting temperature range. The measurement resolution is very low and produces single and dual zone versions, which means that the number of photosensitive areas can be one or two. The below Figure 25 is the MLX90614 standard version.

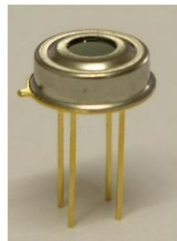


Figure 25. MLX90614 [28]

Unlike usual infrared thermometers or infrared sensors, the MLX90614 uses digital PWM (Pulse Width Modulation) and SMBus (System Management Bus) for output. So, the output is the value of the temperature. Therefore, we can tell the temperature directly without any calibration or any measurement equation. In this project, the MLX90614-BAA is used for sensing infrared. The input supply voltage is 3 volts, the supply current is a maximum of 2mA and FOV is a standard version which have 0 degree of peak zone and 90 degree of width zone. There are several version of IR sensor which has various FOV value. So, the user can select to proper one for their objective considering distance, price, etc.

4.3 Telecommunication module - NRF24L01

For transmitting and receiving the temperature data produced by the infrared thermometer sensor, an NRF24L01 is used in this study. The below Figure 26 is the NRF24L01 standard module.



Figure 26. NRF24L01 [29]

The NRF24L01 is a transceiver module which is produced by Nordic Semiconductor company. This module is a single chip GFSK transceiver. GFSK stands for “Gaussian frequency-shift keying” which is a type of FSK method that uses a Gaussian filter to convert 1 as positive biased and 0 as negative biased. This module uses 2.4GHz and it has 13 channels from 1 to 13 in Finland. Typical supply voltage (VDD) is 3.0 volts and supply current is 11.3mA, which makes it suitable for use with an Arduino.

5 Design of the Prototype

5.1 Flow Diagram

The objective of this study was to make a prototype that is a complete operating system from sensing to alarm by using TEG technology and a telecommunication module for the achievement of early sensing and early stage suppression in a place where there is no installed electrical device or equipment such as an electrical line. Although the main objective of the principle component was to use TEG technology, the secondary component using telecommunication was also important for achieving the goal. This secondary component will use IR sensing, wireless communication (2.4 GHz), and an Arduino. As shown in Figure 27, if a wildfire breaks out, the TEG would generate the voltage to operate the Arduino. If the Arduino turns on, the information about the temperature at the location of the wildfire would be collected by the IR sensor and this information would be transmitted by the transmitter. As a result, the emergency department would be alerted to check on the situation at that location in the deep forest.

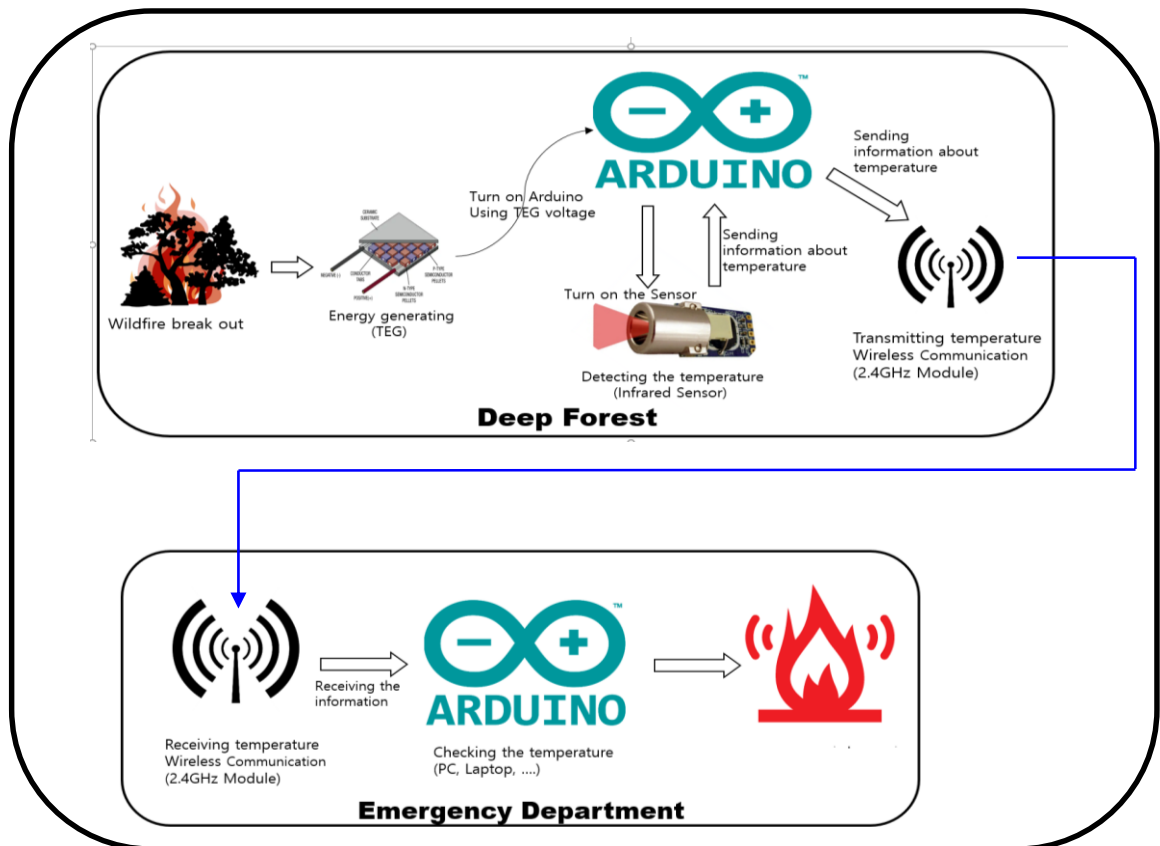


Figure 27. Fire alarm system flow diagram

5.2 3D Structure

Before making a real prototype, a 3D model for checking the outline was made. Program '123D Design' was used when making the 3D model. Figure 28 is a 3D figure of the components that make up the prototype.

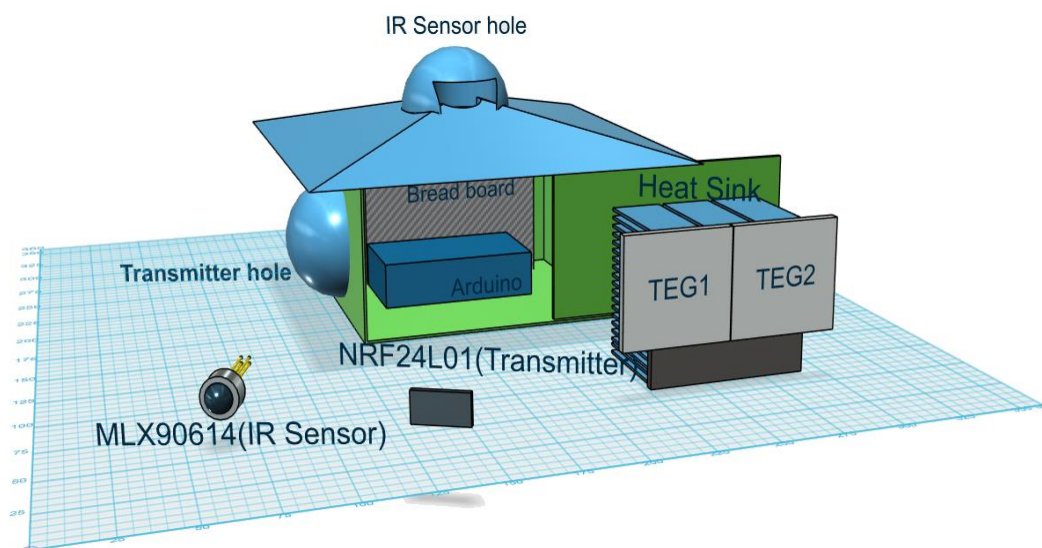


Figure 28. Components of the prototype

In the prototype room, six components were used: IR sensor, breadboard, TEG, Arduino, heat sink, and telecommunication module. Since all of the components are electrical components, to prevent the absorption of rain, plastic was used for making the prototype. It also needed a roof to prevent water getting inside. In order to get a wide detection range, the IR sensor was situated on the top side of the prototype.

The prototype has two holes which are used for an IR camera and a telecommunication module. Since hot material (such as a wildfire) is expected to occur in front of the prototype to generate the voltage, the hole for telecommunication is situated on the left side of the prototype toward the back. The real prototype pictures are given in the Appendices.

5.3 Arduino Wiring Diagram

As shown in Figure 29, since signal is needed for transmitting and receiving, two Arduinos are used. Transceivers use digital SPI communication; therefore, the transmitter and the receiver have to connect to the digital pin and three volts have to be applied to the module because the module's typical supply voltage is 3 volts. If the module is connected to a 5-volt pin, the module could break. The infrared sensor (MLX90614) uses serial communication with the Arduino and the sensor output is an analog type, therefore the data line has to be connected to the analog pin. And unlike the transceiver, the typical input voltage is 5 volts, so it has to be connected to a 5-volt pin.

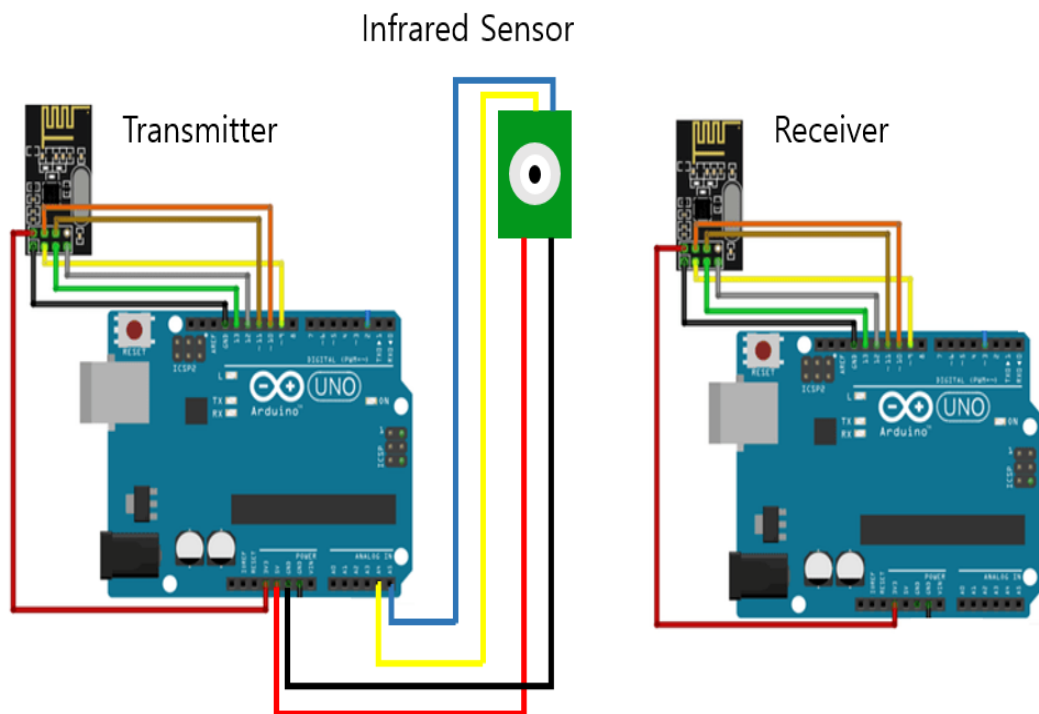


Figure 29. The wire connection between the Arduino Uno and components

The main codes of operation are serial operation and radio operation. So, when setting up the mode of operation, the serial mode and radio mode are operated alternately. The codes are given in the Appendices.

5.4 Generated Voltage and Current

Table 2. Output voltage generation by temperature variation using oven temperature

| One TEG | | | |
|-----------------|----------|------------------------|---------|
| Cold side | Hot side | Temperature difference | Voltage |
| 37 | 44 | 7 | 0.062 |
| 8 | 44 | 36 | 0.134 |
| 8 | 65 | 57 | 0.196 |
| 9 | 126 | 117 | 0.587 |
| 37 | 160 | 123 | 0.38 |
| 2 | 126 | 124 | 1.25 |
| 37 | 177 | 140 | 1.031 |
| 3 | 169 | 166 | 1.78 |
| 6 | 216 | 210 | 2.02 |
| Two TEGs | | | |
| Cold side | Hot side | Temperature difference | Voltage |
| 8 | 110 | 102 | 2.35 |
| 56 | 211 | 155 | 0.89 |
| 8 | 180 | 172 | 3.47 |
| 8 | 210 | 202 | 4.82 |

Theoretical facts can be proved by these Table 2 results. First, the higher temperature at the hot side generates the higher voltage. This is because the higher voltage has more molecules which means higher velocity using the Maxwell-Boltzmann distribution equation (1). This table 2 presents the linear characteristic of the generator as equation (7). A greater temperature gradient generates more voltage. As Figure 24 shows, due to the series connection of two TEGs, more voltage is generated than just using one TEG. In addition, this table presents the characteristic of the thermal conductivity of TEG material in the equation of ZT (eq. 12) as well.

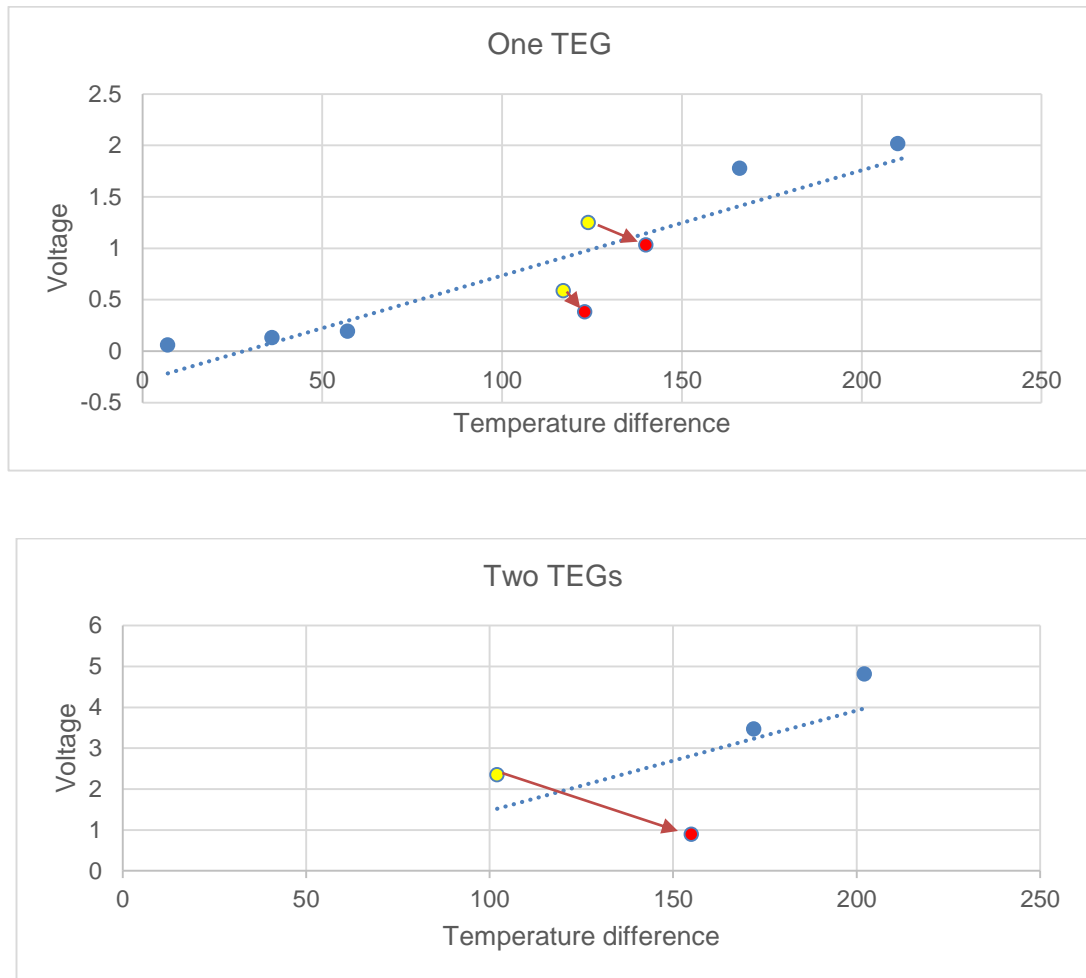


Figure 30. Graphs of generated voltage depend on different temperature differences

Among the many factors that determine the efficiency of a TEG (referred to as ZT), thermal conductivity (k) is the main factor of a material to generate the amount of output voltage in the equation (11,12). The nominal ZT of this TEG is 0.73. According to ZT standards, material which has $ZT=1$ is considered good. However, since this module is an ordinary commercial product, material which has low thermal conductivity is not being used.

In Figure 30, even though the temperature gradient of the red dots is bigger than that of the yellow dots, the output voltage is lower than that of the yellow dots. This is because of high thermal conductivity. When those values were measured, the condition of the temperature of the TEG surface was changing rapidly. When the yellow dot was measured, ice was used to cool down the temperature. On the other hand, when the red dot was measured, no material was used to cool down the cold side. Therefore, although the surface temperature was measured at the cold side (as was done for Table 2), the actual inner temperature was not as low as that used for Table 2. Because the thermal

conductivity of this TEG is very high, the high temperature is conducted very quickly to the cold side from the hot side.

Table 3. Output current generation by temperature variation using oven temperature

| Series connection | | | |
|---------------------|----------|------------------------|------------|
| Cold side | Hot side | Temperature difference | Current(A) |
| 8 | 85 | 77 | 0.52 |
| 8 | 133 | 125 | 0.78 |
| 8 | 146 | 138 | 0.80 |
| 8 | 162 | 154 | 0.82 |
| 8 | 188 | 180 | 0.87 |
| Parallel connection | | | |
| Cold side | Hot side | Temperature difference | Current(A) |
| 8 | 50 | 42 | 0.89 |
| 8 | 109 | 101 | 1.22 |
| 8 | 180 | 172 | 1.65 |
| 8 | 205 | 197 | 2.02 |

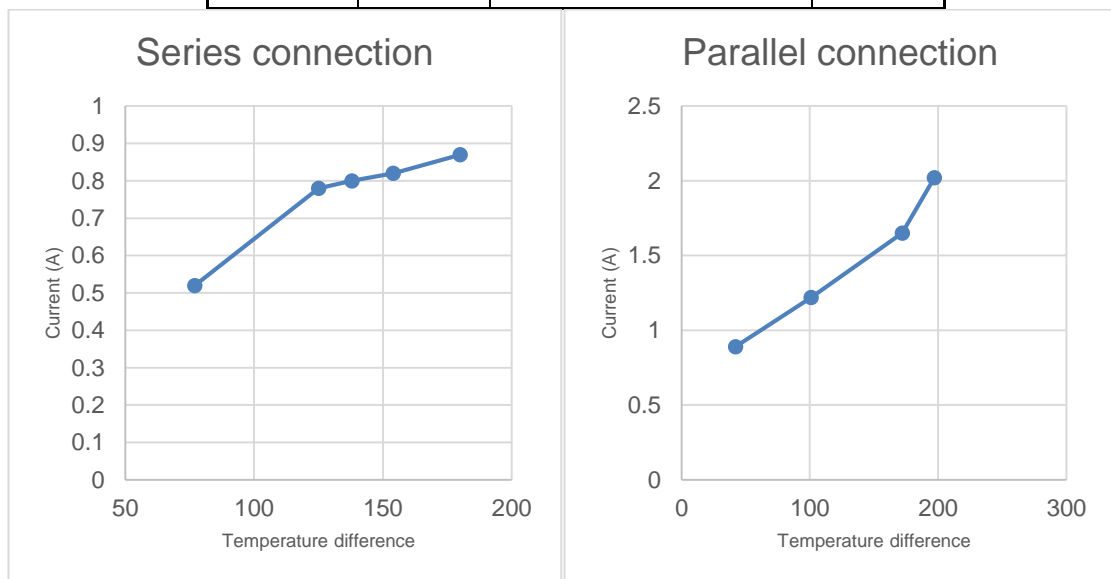


Figure 31. Graphs of generated current depend on different temperature differences

In Figure 31 and Table 3, the generated current depends on temperature differences using two different connection methods. As mentioned in Figure 24, in the parallel connection method, the current was measured to be about two times greater. However, even

if using the parallel connection makes more current available, because using the boost-converter module makes for safer operation, the series connection is more suitable.

5.5 Circuit of the Prototype

For getting high enough voltage (around 12V) and stable current in order to operate the Arduino Uno, a boost-converter evaluation module (TLV61046A) was used.

Table 4. TLV61046A evaluation module performance specifications

| Specification | Test Condition | MIN | TYPE | MAX | UNIT |
|----------------|---------------------------|-----|------|------|------|
| Input voltage | | 1.8 | 3.6 | 5.5 | V |
| Output voltage | VIN = 3.6 V, IOUT = 0.1 A | | 12 | | V |
| Output current | VIN = 3.6 V, VOUT = 12 V | | | 0.15 | A |

As shown in Table 4, the output voltage is fixed with 12V in the evaluation module. Since the supply input voltage of the Arduino Uno is 7V~15V and the NRF24L01 and the MLX90614 use 1mA for operating, this module is the most suitable converter module.

As shown in Figure 32, the fixed output voltage(12V) can be used by the boost-converter.

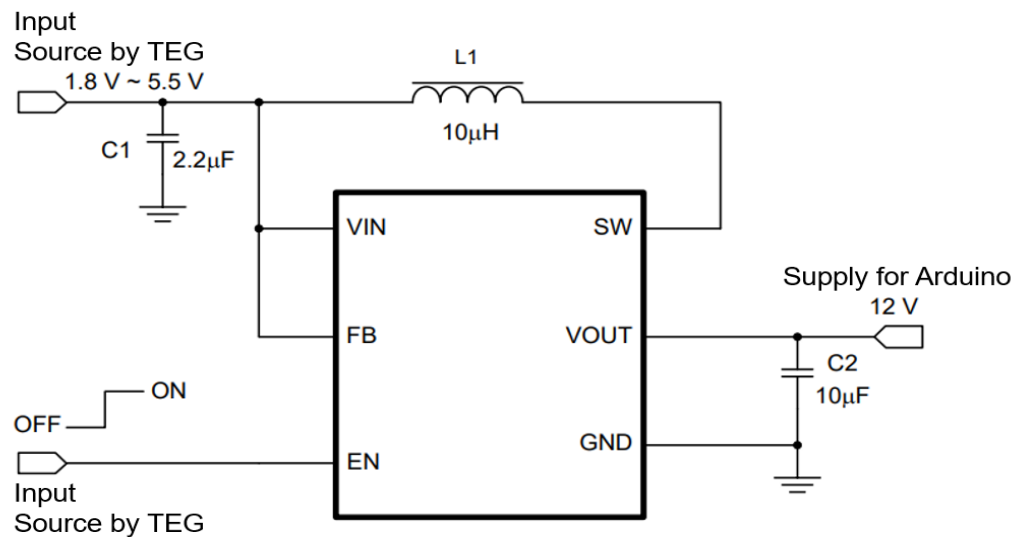


Figure 32. Fixed 12V output voltage with TLV61046A boost-converter [30]

In Figure 32, the output current is 50mA so that amount of current is enough to operate the sensor and telecommunication module fully. When the output current was measured, the 50~100mA was measured depending on the temperature variation.

6 Practical Point of View

6.1 Cost Analysis of the Prototype

One of the project goals was to create an affordable prototype. Therefore, a cost analysis is necessary to estimate the future production price per unit of the prototype. As shown in Table 5, the cost of one unit is € 36.13. Although the total cost of components per one unit is not high, since many of the prototypes are needed, the total cost has to be reduced. Among the components, the heat sinks make up a big part of the total cost, which is 26% of total cost. The NRF24L01+ also takes a big part, which is 39% of the total cost. So, the heat sinks and the telecommunication module would have to be changed to lower the cost product.

Table 5. Device cost by component

| Component | Vendor | Cost/Unit (€) | Quantity | Total Cost (€) |
|---|---------------------------------|---------------|----------|----------------|
| NRF24L01+ (Transceiver & Antenna) | Nordic Semiconductor (e-bay) | 13.99 | 1 | 13.99 |
| MLX90614 (IR Sensor) | Melexis (e-bay) | 2.62 | 1 | 2.62 |
| Arduino Uno (Can be switched to PCB) | Arduino (e-bay) | 3.05 | 1 | 3.05 |
| TEG | Unbranded/Generic (e-bay) | 2.35 | 2 | 2.35 |
| TLV61046A (Boost converter) | Texas Instrument (Farnell) | 0.99 | 1 | 0.99 |
| Heat Sink | Fisher Elektronik (Farnell) | 9.27 | 1 | 9.27 |
| Bread board | Unbranded/Generic (e-bay) | 0.84 | 1 | 0.84 |
| Capacitor | Farnell | 0.01 | 2 | 0.01 |
| Inductor | Farnell | 0.01 | 1 | 0.01 |
| Other (3D Print Case, Wire) | N/A | N/A | N/A | 3.00 |
| Total | | | | 36.13 |

6.2 Strengths and Weaknesses

Strength 1. Does not need electrical source

Officially, in Finland, there are 154 public campsites. If private campsites are added, the total would be increased.[31] In addition, in the US and Canada, there are 13,000 public campsites and innumerable private campsites exist.[32] Especially in the US, there are many campsites with no electricity. So, at those places, the prototype is appropriate to use. The first strength of the prototype is that it can be used regardless of the location. Literally, the prototype can be operated everywhere if the area of the location is small in size.

Strength 2. Low initial cost

One of the problems of wildfire detection systems is the price. Especially, a complete wildfire detection system is too much for a single individual to afford. However, this prototype's cost is much less than other systems or prototypes. Above all, the prototype does not have any other installation charges such as for facilities or equipment. So, this prototype is suitable for individual users.

Strength 3. Diverse utilization

If users want to use various modes or various options, this prototype can be modified very easily because the microcontroller of this prototype is an Arduino Uno. Therefore, there are a lot of options that a user can choose for their preference. For example, if there are a lot of people who want to use this prototype with an added GPS module, the prototype can be modified. And a user could even choose their own version if there were a lot of prototype options. So, it could easily be developed to be a multiple-application prototype.

Even though there are some strengths, this module has many weaknesses and limitations that still need to be resolved.

Weakness 1. Only operates in limited conditions

One of the most vulnerable weaknesses is the operation conditions of this prototype. For the entire prototype (i.e. telecommunication module, sensor, especially the converter module) to operate, the TEG has to generate sufficient voltage. This means that the TEG will have to generate almost the maximum voltage with an ordinary (commercial) TEG. If the temperature condition requirement of the TEG can't be met, it cannot generate

sufficient voltage. So, the whole prototype could not operate, even when using the boost-converter module. So, the result would be that the whole system doesn't work.

Weakness 2. Probability of the being broken by temperature and humidity

Generally, the prototype can be used in a forest. The temperature inside forests is much lower than in other residential places. Especially in winter, there can be expect to be a lot of problems because of the temperature. For example, the temperature range of the Arduino Uno is only -40 to 85 degrees Celsius and generally electrical components cannot be operated in extreme conditions. Also, in Finland even in April and May there is sometimes snow. If the temperature falls below the range, the whole system might be broken. Therefore, in order to prevent the breakdown of the prototype, the prototype would have to be picked up every winter season.

Weakness 3. Limitation of the FOV

Generally, commercial IR sensors have a low FOV, and because of that, the IR sensor might not correctly detect the location of the wildfire. FOV is the detection angle range of a sensor. The FOV of an MLX90614 is -80 degrees to 80 degrees, but that is its maximum range. The range which can detect reliable measured temperature is -36 degrees to 36 degrees and that range is called the "width zone". So, the FOV is too narrow to detect the temperature accurately.

Weaknesses 4. Insufficient voltage generated by TEG

Not only is the ordinary commercial TEG not composed of high-doped semiconductors, but the material of the TEG is also not a suitable material which can generate the amount of voltage needed. Above all, the TEG can be damaged easily by humidity and ice because it is composed high-doped semiconductor. Because of this reason, the TEG would have to be replaced many times.

Weaknesses 5. Telecommunication range

If the many problems above are solved, the greatest weak point of this module is the telecommunication range. In a forest, there are a lot of obstacles to communication between the devices such as trees, water, animals and so on. Because of this problem,

even though the TEG generates sufficient voltage, the telecommunication would not operate. Also, the maximum range of a 2.4GHz NRF24L01+ with antenna is 1.1 km in the open air. Therefore, a large number of prototypes would be needed to cover a big forest.

6.3 Next Version

As mentioned in the previous section, there are a lot of problems which have to be solved for general prototype production.

1. Ways for solving the limited operating conditions

Voltage can be generated by the TEG in limited conditions. Above all, making a greater temperature difference condition between the hot side and the cold side is a problem to be solved. So, for getting a greater temperature difference between the two sides, other ways have to be figured out to cool down without using the heatsink. The heatsink is used to cool down the cold side of the TEG in this version. But it is not enough to cool it down as much as is needed. Changing the structure of the TEG to use water (such as rain) to make something like a liquid CPU cooler would help to create a sufficient temperature difference.

2. Ways for solving the impact of the environment

There are a lot of obstacles and unpredictable events in the forest, such as being attacked by animals. Even if the prototype is taken into consideration when making the prototype, the components are vulnerable to humidity and temperature. Especially, since the sensor and telecommunication module are electrical components, optimization about the structure of the prototype is needed for preventing the impact of the environment. Therefore, when the prototype is produced, damp-proof packaging and techniques which can ensure a constant temperature for the electrical components are needed.

3. How to increase the FOV

Among the various processes of this prototype system, since the main role of the temperature sensor is checking an object's temperature and determining whether it is a fire

or an animal, precision measurement is not needed. Therefore, other sorts of temperature sensors could be used. The MLX90614 is a non-contact sensor, but contact sensors could be another good option just to check an object's temperature. In this version of the prototype, the single zone MLX90614 is used, but if it is changed to dual zone, a wider range of place could be measured because of the wider FOV.

4. Ways for solving the problem of not enough voltage supply

To operate the whole system, sufficient electrical sources are needed. Especially, sufficient voltage and current are essential for communication. But generally, commercial TEGs and affordable TEGs cannot generate enough voltage. The reason why these TEGs cannot generate much of an electrical source is the material of these TEGs. Therefore, to make low thermal conduction, the material of the TEG would have to be changed to a low ZT material. Or switching to a TEG which has a low ZT could be the other option. To get a stable voltage supply, other energy harvesting technologies could be another option, such as a solar panel or a wind turbine to generate the voltage. However, the location where this prototype is to be used is a forest. So, the specifics of the situation and case have to be considered when changing the electrical source. For example, if a solar panel is used, tree leaves could cover the panel and generate shade.

5. Ways for improving the communication distance

Using a 2.4GHz band for communication has some advantages (such as standard of frequency, worldwide allocation, high data rate), making the radio design easier and so on. Although there are advantages, the disadvantages of this frequency band are pretty fatal when using this frequency band in the forest. One of the fatal disadvantages for this module is the short communication distance compared to lower frequencies. Obviously, in the forest, as long as the telecommunication distance needs are met, the total cost of the system can be reduced. However, 2.4GHz is not suitable from that point of view. The way to solve this problem is to change to a telecommunication module which uses a low-frequency band. For example, if 868MHz or a lower low-frequency band such as 433MHz were used, this would help to solve the distance problem. Also, for covering a wide forest, the net system shown below in Figure 33 would be helpful.

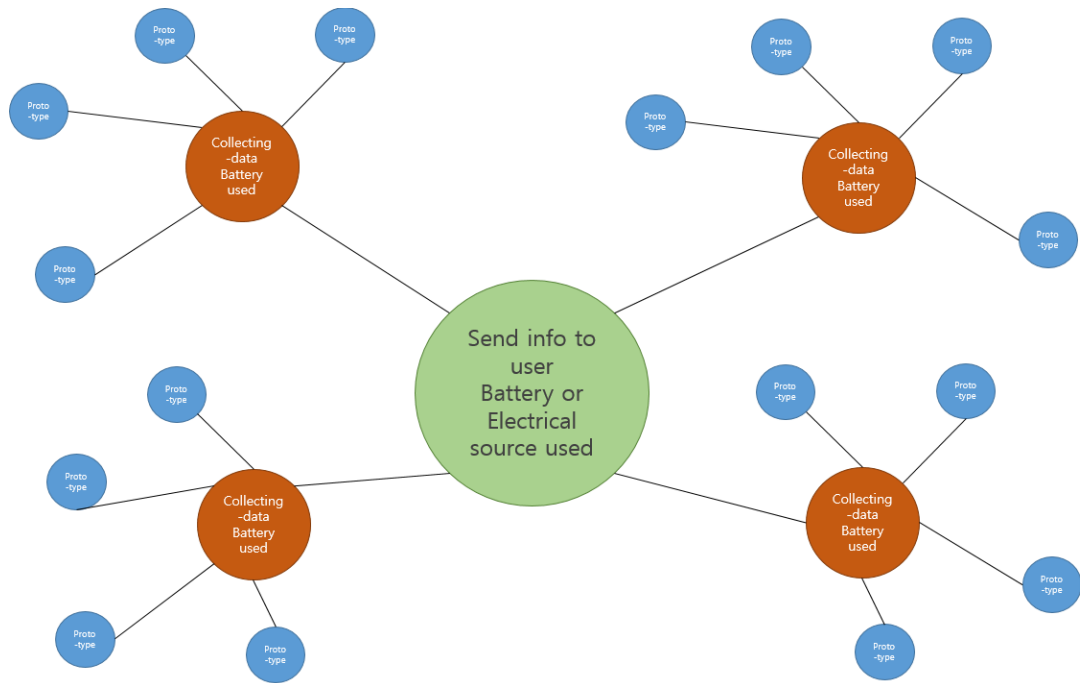


Figure 33. Three-stage net system

As shown in Figure 33, there are three stages. The first and second stages are base stations. Base stations use a battery or electrical source, unlike the end stages which use a TEG to generate voltage. The role of the first stage (green in Figure 34) is to continuously send the information received from the second stage to the user. The role of the second stage (orange in the above figure) is to collect data from the end stage (if it is operating and transmitting data) and send that data to the first stage. So, the three-stage net system could be helpful to cover a wide field or a wide range of forest.

7 Conclusion

The main goal of this project was generating voltage, detecting temperature, and transmitting and receiving data. The voltage tasks (generating voltage using a TEG, amplifying voltage to operate the Arduino using a boost-converter, and adjusting the current to use the sensor and telecommunication modules) were solved. Also, the process for transmitting and receiving temperature data operated well with optimized C code. Therefore, the prototype was successful in relation to the first objective of the project.

However, a lot of problems and weaknesses were identified during the experiment. Above all, the main problem was instability of operation. The prototype cannot operate

without a special case. For example, as mentioned before, the TEG (which is a commercial product) cannot generate sufficient voltage in the usual case. And practical waterproof and damp-proof methods to protect the prototype were not considered during the design of the prototype structure. In addition, the total cost of the 3D model plastic was not taken into consideration.

Although there were a lot of weaknesses with this prototype, this prototype has strengths as well. Above all, flexible options and convenience are one of the main strengths. For example, this prototype can be used in many places such as a campsite or the deep forest. Literally, location is no obstacle to use this prototype. Besides, the size and weight are not big and heavy, and additional installation equipment is not needed. The other strength of this prototype is that this prototype can be easily modified with the next version. And the user can easily choose options and select what they want to use with this prototype.

In this way, this prototype has strengths and weaknesses and should be viewed as just the first version prototype. Therefore, aspects that show up as weakness that have to be solved were left for later versions. For example, the first thing to do next is to solve the problem of a stable voltage supply as this aspect of the prototype has to be upgraded in the next version. Therefore, the more updates and the more modifications, the better the prototype will be. As a result, I hope that this prototype will be helpful in reducing big wildfires and disasters in nature.

References

- 1 Thomas Nilsen. (2018). Forest fire spreads across border from Russia to Lapland, The Barents Observer, pp. A1 <https://thebarentsobserver.com/en/borders/2018/07/forest-fire-spreads-across-border-russia-lapland>.
- 2 Rhee Min Woo, Douglas Gong, Karen Tan, Thomas Chan, Wang Niyou, Tan Geok Bin. (2015), Energy Harvesting for IOT, pp. 48, <https://www.slideshare.net/Funk98/energy-harvesting-for-iot>
- 3 Wikipedia.org. (2018). Thermoelectric Generator. [online]. Available at: https://en.wikipedia.org/wiki/Thermoelectric_generator/ [Accessed 5 Oct. 2018]
- 4 S. M. Sze, Kwok K. Ng. (2006). Physics of Semiconductor Device. Hoboken: Wiley-Interscience pp. 748.
- 5 Aimagin.com. (2018). Thermocouple. [online]. Available at: <http://aimagin.com/blog/how-to-read-thermocouples/> [Accessed 5 Oct. 2018]
- 6 Michael C. Petty, (2007), 'Scope of Molecular Electronics' Molecular Electronics. 3rd ed. Hoboken: Wiley-Interscience, pp.65.
- 7 Libretexts.org. (2018). *The Maxwell-Boltzmann distribution*. [online]. Available at: [https://phys.libretexts.org/TextBooks_and_TextMaps/University_Physics/Book%3A_University_Physics_\(OpenStax\)/Map%3A_University_Physics_II_-_Thermodynamics%2C_Electricity%2C_and_Magnetism_\(OpenStax\)/2%3A_The_Kinetic_Theory_of_Gases/2.4%3A_Distribution_of_Molecular_Speeds/](https://phys.libretexts.org/TextBooks_and_TextMaps/University_Physics/Book%3A_University_Physics_(OpenStax)/Map%3A_University_Physics_II_-_Thermodynamics%2C_Electricity%2C_and_Magnetism_(OpenStax)/2%3A_The_Kinetic_Theory_of_Gases/2.4%3A_Distribution_of_Molecular_Speeds/) [Accessed 5 Oct. 2018].
- 8 Introductory Chemistry.com. (2018). 14.3 Application of Redox Reactions: Voltaic Cells. Available at: https://saylordotorg.github.io/text_introductory-chemistry/s18-03-applications-of-redox-reaction.html/ [Accessed 5 Oct. 2018]
- 9 Wayne M. Saslow. (2002). Electricity, Magnetism and Light. Amsterdam: Elsevier. pp. 305
- 10 Taylor Sparks. (2013). How do thermoelectrics work? [online]. Available at: <https://pubweb.eng.utah.edu/~sparks/how-do-thermoelectrics-work.html/> [Accessed 30 Nov. 2018]
- 11 Wikipedia.org. (2018). Seebeck coefficient. [online]. Available at: https://en.wikipedia.org/wiki/Seebeck_coefficient/ [Accessed 5 Oct. 2018]
- 12 Chegg Study.com. (2018). Question: Relative Seebeck coefficients for some material combination. [online]. Available at: <https://www.chegg.com/homework->

- help/questions-and-answers/relative-see-beck-coefficients-material-combinations-emf-alpha-t2-alpha-t-emfcomp-mu-v-q22613903/ [Accessed 10 Oct. 2018]
- 13 S. M. Sze. (1994). Semiconductor Sensors. Hoboken: Wiley-Interscience. pp.219-279
 - 14 W. Chr. Germs. (2013). Moving charged particles in fluctuating and disordered energy landscapes. Ph.D. thesis. Eindhoven University of Technology, pp. 66, 70, 81
 - 15 Molan Li. (2011). Thermoelectric-Generator-Based DC-DC Conversion Network for Automotive Applications. Master Thesis. KTH Information and Communication Technology
 - 16 G. Jeffrey Snyder and Eric S. Toberer. (2008). Complex Thermoelectric Materials. Journal of Nature Materials 7, [online] pp. 112., Available at: <http://thermoelectrics.matsci.northwestern.edu/thermoelectrics/index.html> [Accessed 11 Oct. 2018]
 - 17 A. Takezawa, M. Kitamura. (2012). Geometrical design of thermoelectric generators based on topology optimization. [online]. Available at: <https://home.hiroshima-u.ac.jp/akihiro/thermoEle.html> [Accessed 1 Nov. 2018]
 - 18 Antonino Proto, Daniele Bibbo, and Martin Cerny. (2018). Thermal Energy Harvesting on the Bodily Surfaces of Arms and Legs through a Wearable Thermoelectric Generator. MDPI sensors, pp. 4.
 - 19 Andrea Montecucco. (2014). Efficiently Maximising Power Generation from Thermoelectric Generators. PhD Thesis. University of Glasgow. pp. 26
 - 20 leilaxx.com. (2015). Tips to take pictures of ghost. [online]. Available at: <http://leilaxx.blogspot.com/2015/10/tips-to-take-pictures-of-ghost.html> [Accessed 1 Nov. 2018]
 - 21 Wikipedia.org. (2018). Plank's law. [online]. Available at: https://en.wikipedia.org/wiki/Planck%27s_law/ [Accessed 25 Oct. 2018]
 - 22 Ceramix.com (2018). Fundamentals of IR [online]. Available at: <https://www.ceramicx.com/infrared-heat/> [Accessed 25 Oct. 2018]
 - 23 Chen Chengying, Yong Hei. (2014). A-55dB SNDR, 2.2-mW double chopper-stabilized analog front-end for a thermopile sensor. Journal of Semiconductors, [online] pp. 055003-2. Available at: https://www.researchgate.net/publication/262455098_A_55-dB_SNDR_22-mW_double_chopper-stabilized_analog_front-end_for_a_thermopile_sensor/download/ [Accessed 1 Nov. 2018]

- 24 HAMAMATSU.com. Thermal detectors. [online]. pp. 3. Available at: https://www.hamamatsu.com/resources/pdf/ssd/e07_handbook_Thermal_detectors.pdf [Accessed 11 Oct. 2018]
- 25 Marlow.com. 12-6 Datasheet. [online]. pp. 1. Available at: https://cdn2.hubspot.net/hubfs/547732/Data_Sheets/TG12-6.pdf [Accessed 03 Nov. 2018]
- 26 Marlow.com. 12-6 Datasheet. [online]. pp. 2. Available at: https://cdn2.hubspot.net/hubfs/547732/Data_Sheets/TG12-6.pdf [Accessed 03 Nov. 2018]
- 27 Thermocoolcorp.com. Bonded Fin Heat Sinks. [online]. pp. 1. Available at: <http://thermocoolcorp.com/project/bonded-fins/> [Accessed 03 Nov. 2018]
- 28 Sparkfun.com. MLX90614 family Datasheet. [online]. pp. 1. Available at: https://www.sparkfun.com/datasheets/Sensors/Temperature/MLX90614_rev001.pdf [Accessed 03 Nov. 2018]
- 29 indiamart.com. NRF24L01 2.4GHz Antenna Wireless Data Transmission Module. [online]. Available at : <https://www.indiamart.com/proddetail/nrf24l01-2-4ghz-antenna-wireless-data-transmission-module-17424160033.html> [Accessed 04 Nov. 2018]
- 30 ti.com. TLV61046A Datasheet. [online]. pp. 8.3. Available at: <http://www.ti.com/lit/ds/slvsd82a/slvsd82a.pdf> [Accessed 17 Jan. 2019]
- 31 camping.info. Finland Campsites. [online]. Available at: <https://en.camping.info/finland/campsites/> [Accessed 17 Jan. 2019]
- 32 uscampground.info. US campground. [online]. Available at: <http://www.uscampgrounds.info/> [Accessed 17 Jan. 2019]

Transmitting code

```
#include <i2cmaster.h> //
#include <SPI.h>
#include <nRF24L01.h>
#include <RF24.h>
RF24 radio(7, 8);
const byte address[6] = "00001";

struct package
{
  float celcius;
  float fahrenheit;
};

typedef struct package Package;
Package data;

void setup() {

  //*****NRF24L01 Setup*****
  Serial.begin(9600);
  i2c_init();
  PORTC = (1 << PORTC4) | (1 << PORTC5);
  radio.begin();
  radio.openWritingPipe(address);
  radio.setPALevel(RF24_PA_MIN);
  radio.stopListening();
}

void loop(){
  readSensor();
  Serial.println(data.celcius);
  radio.write(&data, sizeof(data)) ;
  delay(1000);
}

void readSensor()
{
  int dev = 0x5A<<1;
  int data_low = 0;
  int data_high = 0;
  int pec = 0;

  i2c_start_wait(dev+I2C_WRITE);
```

```
i2c_write(0x07);

i2c_rep_start(dev+I2C_READ);
data_low = i2c_readAck();
data_high = i2c_readAck();
pec = i2c_readNak();
i2c_stop();
double tempData = 0x0000;
double tempFactor = 0.02; // 0.02

tempData = (double)((((data_high & 0x007F) << 8) + data_low));
tempData = (tempData * tempFactor)-0.01;

float celcius = tempData - 273.15;
float fahrenheit = (celcius*1.8) + 32;.
data.celcius = celcius;
data.fahrenheit= fahrenheit;
}
```


Receiving Code

```
#include <SPI.h>
#include <nRF24L01.h>
#include <RF24.h>

RF24 radio(7, 8);
const byte address[6] = "00001";
struct package
{
  float celcius;
  float fahrenheit;
};

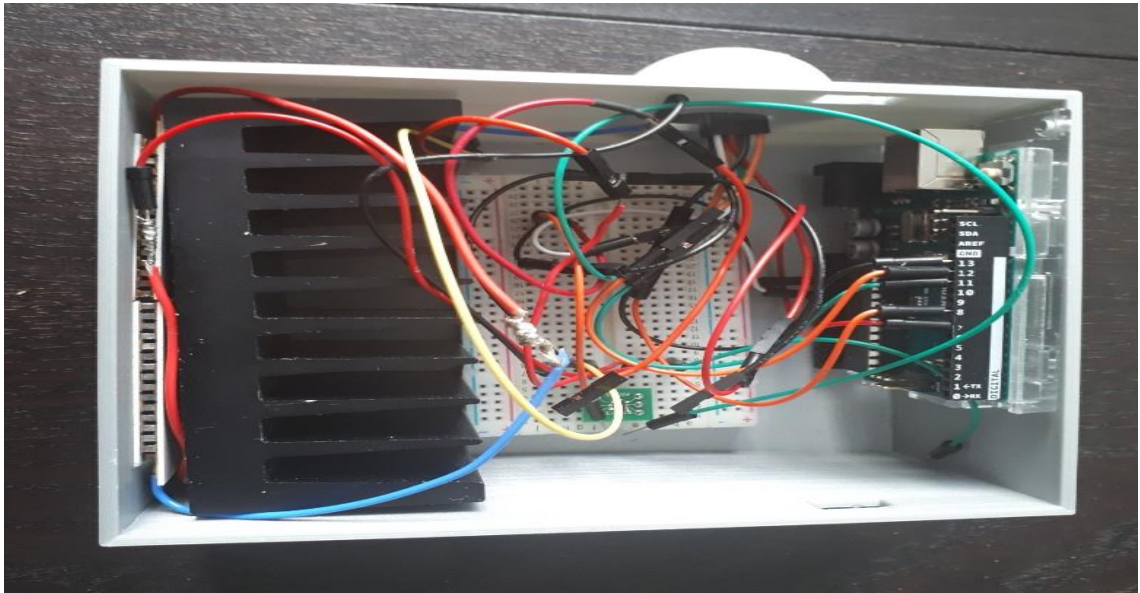
typedef struct package Package;
Package data;

void setup() {
  Serial.begin(9600);
  radio.begin();
  radio.openReadingPipe(0, address);
  radio.setPALevel(RF24_PA_MIN);
  radio.startListening();
}

void loop() {
  if (radio.available()) {
    radio.read(&data, sizeof(data));
    Serial.print("Celcius : "); Serial.print(data.celcius); Serial.print(" ");
    Serial.print("Fahrenheit: "); Serial.println(data.fahrenheit);
  }
}
```

Structure of the Prototype

- The inside



- Front view



- Side view

